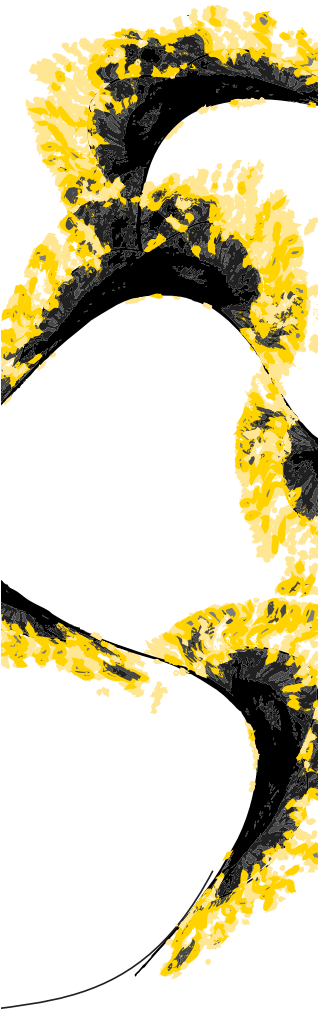

RAM ROBOTICS AND MECHATRONICS

A SOFT ROBOTIC KNEE BRACE FOR IMPROVING KNEE STABILITY IN ANTERIOR CRUCIATE LIGAMENT DEFICIENT PATIENTS

H.M. (Husain) Khambati

MSC ASSIGNMENT

Committee:
dr. ir. J.F. Broenink
dr. ir. H. Naghibi Beidokhti
dr. ir. M. Abayazid
dr. ir. G.D.S. Ludden

October, 2019

Robotics and Mechatronics
EEMathCS
University of Twente
P.O. Box 217
7500 AE Enschede
The Netherlands

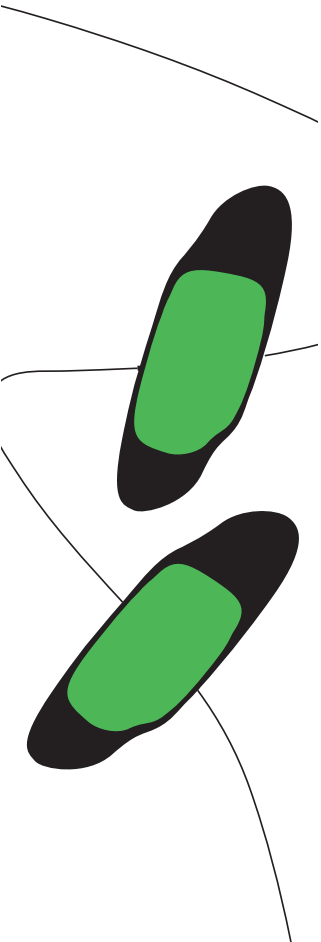

UNIVERSITY OF TWENTE. | TECHMED CENTRE UNIVERSITY OF TWENTE. | DIGITAL SOCIETY INSTITUTE

Summary

The Anterior Cruciate Ligament (ACL) is one of the major stabilizing ligaments present in the synovial knee joint. It is also the most commonly injured ligament, occurring due to sudden twisting of the knee under load. The rupture of the ligament causes a loss of stability in knee allowing for increased motion of the bones. This increased motion raises the risk of knee arthritis or Osteoarthritis (OA) in the years following the injury. Reconstructive surgery is often prescribed to patients with high activity levels such as athletes, whereas patients with low activity levels generally rely only on rehabilitation provided after the injury. Both of the options though viable, do not necessarily reduce the risk of OA.

Knee braces are often prescribed during and after rehabilitation to increase the stability of the knee joint; However, most knee braces often overlook the effect on the underlying passive structures. Evaluating the effect of these braces limits them in their design. To see the effect of these braces an MRI scan of the underlying passive structures is required to asses the strain put on them. To develop a knee brace which can allow us to see the effects put on the passive structures would need a MR compatible actuation design to compensate for the loss of stability.

Pneumatic Artificial Muscle (PAM)s are soft actuators which mimic the basic functionality of the human muscles. These actuators are made of silicon wrapped in a nylon sheath, which make them by design, MR compatible. We design and fabricate these PAMs and integrate them into a knee brace with the aim of reducing the instability caused due to an ACL rupture.

The hamstring muscles group situated behind the thigh, is an important muscle group when it comes to reducing the instability caused by the ACL rupture. We design our brace to assist this muscle group. As such an EMG muscle activation study is performed during a seated hamstring curl exercise and during normal walking to check for a reduction in hamstring activation.

Preface

The work presented in this thesis would not have been possible without the constant guidance of my supervisors, Hamid Naghibi Beidokhti and Momen Abayazid. The finite element simulation highlighted in chapter 6 was done by Hamid.

Henny Kuipers and Sander Smits helped me in fabrication the 3D printed parts and the design of the support structures. The EMG device was borrowed from the TechMEd department at the UT.

I would also like to thank those who participated in my experiments.

Contents

List of Figures

1 Introduction

1.1 What is ACL?

The Anterior Cruciate Ligament (ACL) is one of the two crutiate ligaments that form an 'X' like structure inside the knee joint. These two crutiate ligaments are the anterior and Posterior Cruciate Ligament (PCL). Both of these articulates are present between the femur (upper leg) and tibia (lower leg). The placement of the ACL is such that it prevents the anterior (forward) motion of the tibia along the femur, whereas the PCL prevents the posterior (backwards) motion of the tibia. Both of these ligaments together protect the underlying cartilage by preventing unwanted movement of the two bones. They also provide rotational stability during flexion (bending of the knee). The rupture of the ACL introduces instability in the knee joint in the form of anterior displacement of the tibia with respect to the femur. This motion is termed as Anterior Tibial Translation (ATT).

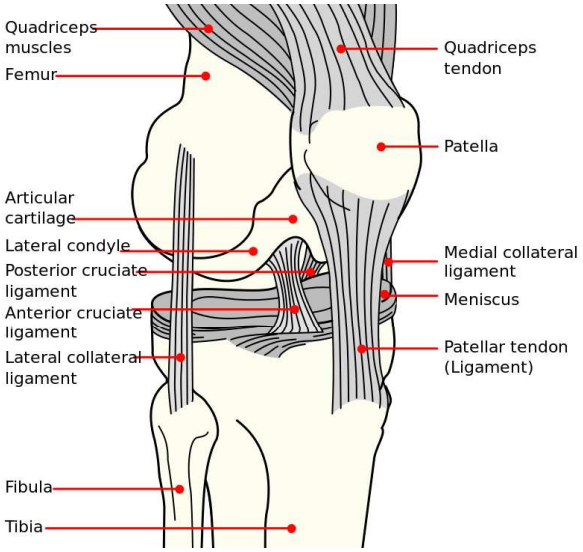

Figure 1.1: The structure of the knee and all surrounding articulates. From Commons (2019)

1.2 ACL Rupture

The ACL is also the most injured ligament of the four present in the knee. The other two being the lateral (outer side) and medial (inner side) collateral ligaments. An ACL rupture is a very common injury among sports where players and athlete stop suddenly and change direction quickly while running or sprinting causing the ligament to stretch and sometimes even tear. This injury can also be caused by sudden jerk or high loading of the knee joint. This usually occurs in high risk pivoting sports when athletes land on a leg and start rotating in the opposite direction (Dargel et al., 2007). In cases of complete rupture, patients with high levels of physical activity sometimes choose to undergo a reconstructive surgery, where the attending surgeons replace the torn ACL. In a few cases, the ligament is only partially torn, despite this surgeons usually prefer reconstructive surgery instead of repairing the ACL (Flandry and Hommel, 2011). This is due to the anatomical structure of the ACL, which consists of two bundles of fibers, which vary their tension based on the angle of flexion of the knee. The blood supply to these bundles are through anastomosis (A cross connection between two blood vessels), as a result any damage to the ACL permanently disrupts the blood supply and it can no longer heal it self (Toy et al., 1995).

1.3 ACL Reconstruction

ACL reconstruction surgery is performed by replacing the torn ligament with a graft taken from the patellar tendon or in some cases the hamstring tendons. Grafts taken from the quadriceps or a synthetic tendon is also an option and is the choice of the attending physician (Cerulli et al., 2013). It is possible for some ACL reconstruction patients to return to their preinjury level of activity after the surgery; However, the ACL cannot be completely replaced by a graft. The surgery consists of drilling sockets in the bones for correct graft placement. The graft is then tightened to the bone using screws.; However, the tightness is not mentioned specifically and is upto the judgment of the attending physician. Unfortunately, ligament reconstruction cannot recreate the anatomical, biological, biomechanical and neurophysiological properties of a native ACL. Many patients also opt for rehabilitation instead of the surgery. In both cases the loss of the ACL is apparent in their movement patterns and kinematics. In both cases the patients have experienced a reduction in their knee function and physical activity.

1.4 Problem statement

The ACL is therefore a crucial ligament for stable movement of the knee. Reconstruction of the ACL though a viable option, yet does not perfectly mimic the function of the ACL. The absence or the lack of a properly functioning ACL causes wearing of the meniscus cartilage (shock absorber present in between bones of the kee joint) present in the knee, which might lead to Osteoarthritis (OA) in the future. Knee braces are readily available which support the knee in such conditions and are often advertised as, being able to improve the stability of the knee joint: However, the efficacy of the knee brace is still not entirely known. These knee braces usually restrict the range of motion of the knee, by placing a hard stop in the knee hinge mechanism to prevent full flexion of the knee joint. In retrospect, the knee braces do tend to stabilize the knee; However, the hard stop at greater angles of flexion may cause a sudden jerks which may cause significant pain to the patient. The efficacy of the knee braces have been examined using either cadaveric specimens or using simulations based on patient data. Very little is seen in terms of examining the articulates surrounding the knee joint while wearing such a brace. To be able to investigate the effects these braces have on ACL rupture patients, it is crucial to follow the movement of the bones in order to assess the strain on the underlying meniscus. Such an examination would require the use of a medical imaging modality of the bones in the knee joint while under the influence of the brace, unfortunately these tests severely limit the design of most knee braces. *Resulting in little to no information about the effect of theses braces on the underlying soft tissues.*

1.5 Research Questions

This assignment aims at developing a functional knee brace for ACL rupture patients to reduce the risk of OA. To this goal we have the following research questions

- We first find *"The biomechanical instability caused by an ACL rupture and how the effects could be reduced?"*.
- We then look into *"How to develop a knee brace which could be used to evaluate the strain on the soft tissues around the knee and the underlying articulates?"*.
- Finally we evaluate *"What is the effect of our soft robotic knee brace on reducing the instability in an ACL ruptured knee?"*.

1.6 Design Requirements

1. The developed brace should be able to reduce the instability caused by an ACL rupture.

2. To prove the efficacy of our soft robotic knee brace we must be able to measure the movement of the bones. Imaging modalities are able to produce high quality images of the underlying bones and are not affected by skin and muscle movements around the bones. Some of the imaging techniques to measure the bone movement are as follows:

    - *CT scan/X-ray imaging:* A computerised tomography (CT) scan are quick and produce high quality images. While X-ray scans are less detailed about the surrounding organs and muscles but are able to generate images of the bones. But both the processes involves the patient being exposed to radiation which is not desirable for testing our knee brace.
    - *Ultrasound imaging:* Ultrasound imaging does not penetrate the bone and can be used to measure the movement of the bones; However the images generated have a low resolution due to the limited range of penetration of the ultrasonic waves. The field of view of the ultrasound image is also limited.
    - *MRI scan:* Magnetic Resonance Imaging (MRI) is non-invasive and radiation free method for generating images of the brain and spinal cord, bones, the heart, blood vessels and different internal organs. As a result MRI scan is a good method for proving the concept of our knee brace. As a result the knee brace should be made MRI compatible.

3. Safety:

    - *Compliance:* The knee brace must not be too rigid as to cause damage to the underlying tissues around the knee joint. The knee brace should not hinder the range of motion of the joint. The actuators used in the knee brace are pneumatic actuators that are made of silicon and provide enough compliance for safe human-machine interaction.
    - *Forces:* The forces produced by the brace must be within medical limitations to avoid damage to the joint. Each of the pneumatic actuators on the brace have a maximum force of upto 50N at 2 bars of pneumatic pressure. A Lachman test is a procedure used by clinicians to evaluate the laxity (looseness of a limb or muscle) of the knee joint. During the test, a force of 120N is applied to the posterior of the tibia to produce an anterior motion. Therefore, two pneumatic actuators are used to provide a maximum force of 100N.
    - *Pressure:* The knee brace should be portable enough to be worn daily. As a result the pressure used to actuate the knee brace is kept at a maximum of 2 bars of pneumatic pressure. This allows the possibility of adding a portable compressor onto the brace, thereby increasing the mobility of our system.

4. The knee brace should be light weight. The optimal load for carrying on a day to day basis is one-third the body weight for human male adults (Haisman, 1988). As a result we consider the weight of the brace to be less than 1kg. This weight limit allows for implementing further systems onto the brace in the future.

5. The design of the brace should not be limited to one type of knee. The structures of the brace should easily be replaceable for different knee sizes.

6. The brace is intended to be worn by patients during their daily lives. The knee brace should not cause skin irritation or any pinching on the skin as it may cause pressure ulcers.

7. Our brace design will not be considering the entire range of motion of the knee, instead we focus our aims on reducing the instability at certain flexion angles.

Table 1.1: Summary of design requirements according to their priority

Requirements	Must have	Should have	Could have	Would have
Functionality: To reduce the instability of an ACL ruptured knee	X			
Safety: For the soft tissues around the knee while wearing the brace	X			
MR Compatibility		X		
Ergonomics: Comfort, Wearability, Customizable			X	
Aesthetics				X

1.7 Thesis Outline

The knee brace is developed for the purpose of trying to reduce the instability caused in the synovial knee joint due to the rupture of the ACL. Reducing the anterior motion of the tibia along the femur serves to protect the underlying meniscus cartilage, thereby lowering the risk for OA in the years following the injury. The actuation required is produced by linear soft actuators, due to their compliant behaviour. The actuators are in the form of Pneumatic Artificial Muscle (PAM), which are able to generate a large range of forces at low pressures. These are some of the factors which make the PAM's suitable for human machine interaction. The fabricated PAMs are integrated into a knee brace with the aim of decreasing the ATT motion We believe that the hamstrings are an important muscle group responsible for reducing the instability following an ACL rupture. A surface EMG test is conducted to verify if the developed brace is able to assist the hamstrings.

2 Literature Survey

2.1 ACL deficiency

The loss of the ligament in Anterior Cruciate Ligament Deficient (ACLD) patients leads to instability in the knee joint due to the ATT movement. The medial meniscus becomes the secondary restraining force to the ATT; However, this puts the meniscus at risk. The posteromedial (posterior and medial side) meniscus strain increases after an ACL tear, which places a high risk of tearing on the meniscus (Lee et al., 2006). This is one of the major causes of OA in patients during the years following the injury. Anterior Cruciate Ligament Reconstructed (ACLR) patients are able to return to normal physical activity after their surgery, while ACLD patients will have to recover their lost stability by training different muscle groups during rehabilitation to try and compensate for the ACL

The patients who have gone through reconstructive surgery also have issues concerning the thin cartilage present in the knee joint. Brandsson et al. has shown a comparison in the kinematics and laxity of the knee joint for patients with a ruptured ACL and patients who have gone through with the reconstruction surgery using the patellar tendon as a graft. They show that reconstruction surgery does not return the kinematics to normal during the entire range of flexion-extension of the knee joint. This is due to the structural differences between the ACL and the patellar tendon graft. The ACL is a fibre of two bundles (Flandry and Hommel, 2011), whereas the patellor tendon is more uniform and straight.

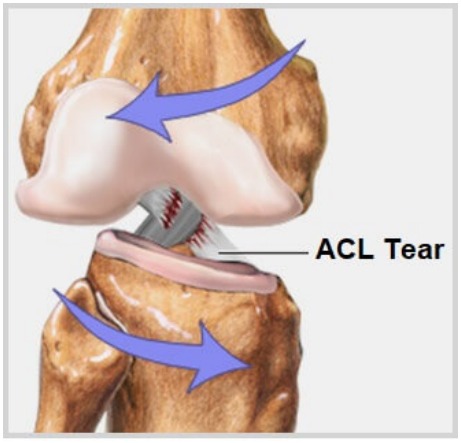

Figure 2.1: ACL rupture. From Wilson (2018)

2.2 Alteration in moving pattern

Studies comparing patients with ruptured ACL to healthy patients have shown the differences in the kinematics of the leg. Slater et al. have mentioned an extensive survey on patients with an ACL rupture. The paper compare patients who have undergone a reconstructive surgery and those who have not. A control group of healthy patients was also introduced. The data used was not only of new patients but of patients who have had time to re-cooperate and have gone through rehabilitation. Their study has shown that ACLD and ACLR patients have reductions in knee flexion angle as compared to the control group. The ACLR patients have a lower reduction in their kinematics compare to the ACLD patients. In both cases we can see the alterations caused by the ACL to the kinematics of the movement of the leg in the frontal and sagittal-plane. They also mention that the rehabilitation process is crucial in regaining the proper kinematics of the knee. The rehabilitation process allows the patient to strengthen their muscles around the knee to provide the stability required for normal kinematics.

Rudolph et al. have also done a similar comparison between patients who have instability in their knees in daily activities (non-copers) and with patients who have overcome their instabilities by utilizing a stabilizing strategy (copers). The copers utilize a strategy where they stiffen their knee joint and also contract their hamstring muscles and quadriceps for better stability. The copers due to this dynamic stiffness are able to walk in a similar manner to a healthy subject. The non-copers have compensated this by reducing the force by which their heel pushes the ground to reduce strain on the joint. This is abnormal gait cycle might reduce the strain on the knee joint but may cause potential damage to articular structures. Rehabilitation right after surgery can help the patients better utilize the stabilizing strategy, such that they can adapt better and can compensate for the loss of the ACL.

2.3 Effect of hamstring muscle group activation on the ATT motion

While executing a specific motion our body utilizes two types of muscle groups. The first muscle group being the agonist muscles, which provide the bulk of the force. The second muscle group being the antagonist muscles which have a low-level of activity but are required for the proper motion of the joints (Hirokawa et al., 1991). When the knee joint is loaded by the quadriceps (agonist muscles) the sensory receptors in the ACL triggers the hamstrings during knee extension for further joint stability (Aagaard et al., 2000. This sensory activation of the ACL is called the hamstring reflex arc. The fast responding reflex arc exists in the mechanoreceptors in the ACL to hamstring muscle group. Bryant et al., 2008 also show that patients who have a torn ACL have lower hamstring torque compared to patients who have gone through reconstructive surgery. They also report a reduction in the ATT due to the activation of the hamstrings in various day to day activities such as walking, squatting and climbing of stairs. The hamstring on contraction provide much needed stability to the knee.

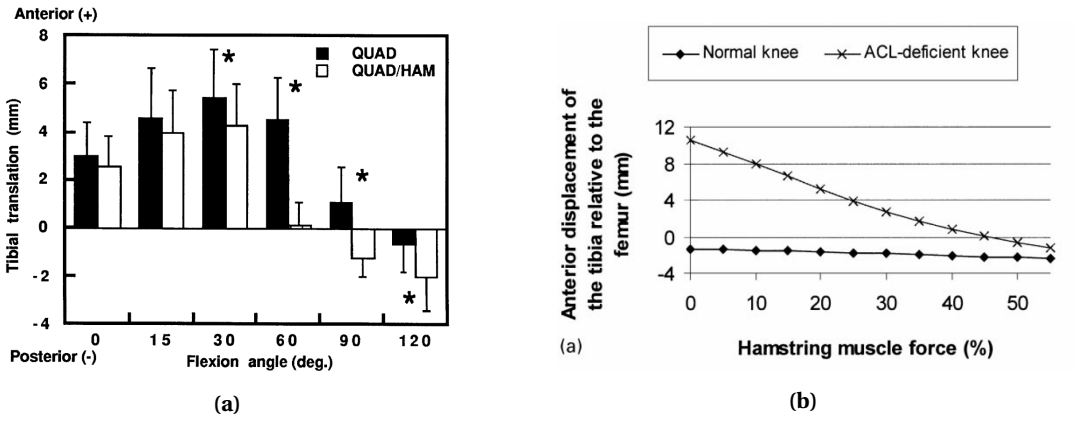

Figure 2.2: Effect of hamstring muscle group on the ATT motion of the knee: a). Anterior Tibial Translation as a function of knee flexion angle as performed on cadaveric human knee specimens. QUAD: Application of 200N quadriceps force, QUAD/HAM: Application of 80N hamstring force with 200N quadriceps forces. From: Li et al., 1999. b). Anterior Tibial Translation as a function of hamstring muscle forces. Comparison is made between a normal knee and ACLD knee on a 2 dimensional anatomical model. From: Liu and Maitland, 2000.

Li et al., 1999 mentions in their paper the effect of quadricep and hamstring co-contraction forces on the ATT movement in an ACLD cadaveric knee. The anterior motion of the tibia was monitored while under the influence of isolated quadricep in-situ forces. Later the addition of hamstring forces showed a decrease in the anterior motion of the tibia. The Fig 2.2a shows the effect of isolated quadricep forces and the effect of quadricep forces with hamstring co-contraction forces on the ATT motion of the ACL deficient cadaveric knee. A similar conclusion is drawn by Liu and Maitland who developed a 2-D analytical knee model to examine the an-

terior motion of the tibia under different levels of hamstring activation. Fig 2.2b shows the result of their model. They show that by increasing the hamstring activation the model is able to exhibit similar behaviour to a healthy patient in terms of the ATT motion.

Hirokawa et al. also mention that the hamstrings do not reduce ATT from 0° to 15° and the most effective reduction is in the range of 15° to 80° of flexion. This is an important function of the hamstring and in the case of an ACL rupture the hamstring reflex arc becomes slower to activate the hamstrings leading to greater ATT. Patients with an ACL rupture during rehabilitation are made to strengthen their hamstring muscles rather than their quadriceps for this very reason.

3 Knee brace

In this chapter we review the different types of knee braces used for medical rehabilitation and injury prevention. The knee braces are classified based on their function to reduce stress on the articulates surrounding the knee joint. We further discuss the effect of knee braces on ligament injuries such as an ACL or PCL rupture. Finally we inspect the different techniques used to evaluate the efficacy of knee braces. Based on the evaluation techniques we can then design our knee brace keeping in mind the effect on the articulates over a long period of time.

3.1 Types of knee braces

1. *Prophylactic knee braces:* Prophylactic knee braces are used to protect the ligaments from injuries. They are generally worn by athletes during contact sports to prevent or reduce the severity of injuries to the ligaments. These braces are generally used to protect the Medial collateral ligament from injuries.

2. *Rehabilitative knee braces:* Rehabilitative knee braces are prescribed to protect the knee ligaments after a recent surgery or injury. These braces help in limiting the movements of the knee to avoid unwanted stresses on the repaired or replaced ligaments.

3. *Unloader/Offloader knee braces:* Unloader braces are prescribed to patients suffering from knee arthritis. Knee arthritis or OA occurs when the thin meniscus cartilage present in the knee joint becomes thin. This results in the bones coming in contact leading to pain and discomfort in the joint. Unloader braces tend to apply a force to the injured side of the arthritic knee preventing bone contact. This relives stresses off of the cartilage preventing further damage. These braces are generally worn by people waiting for a knee replacement surgery.

4. *Functional knee braces:* A functional knee brace is used to support injured knees by enhancing their stability. Following a ligament injury the knee losses some of its stability allowing unwanted motion of the bones, such is the case for an ACL injury. In this thesis we develop a functional knee brace as we intend to regain the stability of the knee joint after an ACL injury.

3.2 Effect of knee braces

Knee braces have been prescribed by therapists to patients suffering from an ACL rupture or those who have gone through the reconstructive surgery. These braces are commonly prescribed to maintain the normal knee stiffness and kinematics of the knee. The braces can be used to reduce the strain on the graft in reconstructed ACL patients or can also be prescribed to ACLD patients to reduce ATT and protect the medial meniscus. These knee braces are most effective at lowering strain in the ACL at low loads.

Tomescu et al. in his article mentions the effect of a dynamically tensioned knee brace in reducing ATT as well as ACL and mensicus strains. They have performed their studies on cadaveric knees and measuring the strain in ACL deficient and complete conditions. They have shown that the strain in the meniscus have been lowered and have also reduced ACL strain during different basic activities such as double and single leg squats and normal gait cycle. LaPrade et al. have compared two types of knee braces for patients suffering from the rupture of the Posterior Cruciate Ligament (PCL). A comparison is made between a static knee brace and a dynamic brace for providing an anterior force to the tibia, which reduces knee laxity in case of a PCL rupture. They conclude on the note that dynamic braces provide more forces across the entire range of motion of the knee in comparison with static knee braces.

Figure 3.1: Different types of available knee braces. a) Prophylactic knee brace from (BraceAbility, 2004). b) Rehabilitative knee brace from (Donjoy, 2019). c) Unloader knee brace from (Orthomen, 2019). d) Functional knee brace from (Carboflex, 2019)

3.3 Evaluation of current knee braces

A review published by Parween et al. on the methods of evaluating the efficacy of unloader knee braces mentions the shortcomings of current knee brace evaluation techniques. These techniques are not limited to only unloader braces but are crucial evaluation methods for medical braces in general. They mention that currently there are different types of evaluating methods such as:

1. *Perception-based:* These are generally questionnaires and visual scores which define the progression or current state of the disease. The patients are asked to provide feedback on the knee braces and the effect on their daily lives. This method is accepted by clinicians but do not provide information about the actual biomechanics of the knee and do not show the effect on the surrounding tissues.

2. *Morphology-based:* These evaluation methods are mostly based on imaging modalities such as MRI, CT scans, X-rays and ultrasounds. This evaluation method provides us with images and models of the surrounding articulates in the knee joint. Being able to inspect the damage to the articulates, the clinician can then assess the stage of progressive OA. This method is used during graft repair or replacement to assess the the effect knee braces in protecting the graft.

3. *Biomechanics-based:* This method evaluates the contraction of surrounding muscles and the firing sequence of the various muscles around the knee to evaluate the efficacy of the knee brace. Biomechanical-based evaluation techniques consist of methods such as 3-D motion analysis during gait, sEMG study for muscle activation patterns and force plate experiments. sEMG study can also show the effect muscle strength has on reducing the instability in the knee. As a result we can then assess the effect of the knee brace in reducing the activation of the muscles or to increase the effect of the muscles to stabilize the knee joint.

3.4 Summary

There is not much in the literature on the effect of knee braces on the surrounding articulates over an extended period of time. Current literature mostly specifies biomechanical based methods of evaluation over morphological methods due to the limitations caused by the various imaging techniques. X-ray and CT scans cannot be used for a lengthy study due to the harmful effects of radiation emitted by the techniques. While MRI scans require the knee braces to be limited to materials that are MRI compatible. Thus limiting the study of dynamic braces due to the incompatibility of standard actuators in a high power magnetic field.

To get a better understanding of the effect our brace will have on the knee joint we design the brace such that, we are able to not only measure the biomechanics of the knee but, also the long term effect of the brace on the surrounding tissues. As a result our design needs to be MRI compatible, which is why we first develop a method for actuating our brace which meets our requirements.

4 Pneumatic Artificial Muscles

In this chapter we discuss the design and fabrication of Pneumatic Artificial Muscle (PAM) for actuation of the brace. We first give a brief explanation on soft actuators followed by the working principles of a pneumatic muscle. We further discuss the required parameters for designing our muscle and also to estimate the amount of force produced by the artificial muscle. Once we have our parameters we then proceed with fabricating our PAM. Attachments are made to integrate the artificial muscle onto the brace. We experimentally validate the force characterization of our artificial muscles as a function of pressure.

4.1 Pneumatic actuators

Pneumatic actuators use the energy stored in compressed gas to create a mechanical motion. The motion can be linear (Andrikopoulos et al., 2011) or rotational Sun et al. (2013). These devices are generally used in robotics and the automation industry, owing to their low weight and compliant behaviour. Pneumatic actuators owe their compliant behaviour to the compressibility of air, which is why these actuators are preferred when there is a need for human machine interaction. Electric motors on the other hand are generally rigid and are made compliant through complicated feedback controllers. A few examples of pneumatic actuators are pneumatic pistons, pneumatic stepper motors and pneumatic engines, Bending actuators. Another actuator which is often used in medical robotics are pneumatic artificial muscles, as they exhibit behaviour similar to the working of a human muscle and have a high force to weight ratio.

Pneumatic artificial muscles are a type of pneumatic actuators which are dependent on the state of their inflation to generate force. Their core is essentially a membrane wrapped in a braided sleeve which contracts axially on inflation. Despite their light weight they are able to generate forces equal to pistons. These are some of the reasons why they are being used in robotics applications. The muscles can be classified on the angle of the braided sleeve. Artificial muscles with a weave angle of 90° are termed as straight fibre muscles and any muscle with an angle other than 90° they are generally termed as McKibben muscles (Carlo Ferraresi et al., 2001).

4.2 McKibben actuator

McKibben actuator is a type of a pneumatic artificial muscle which is composed of a inner latex or silicon bladder which is then covered by a braided mesh sleeve. The actuators works on compressed air or in some cases under hydraulic pressure as well (Mori et al., 2010). The advantage of these over conventional pistons is that there is almost no static friction which does not produce jerks in actuation and are thus better in cases of medical rehabilitation. The muscle itself is hazard-free and causes no pollution or any harmful effects. The actuators also do not utilize any sliding mechanism and can also be used around high magnetic fields. This allows for testing of the system in an MRI which would allow for a better validation of our test result.

The working of actuator is based on the inflation of the inner elastomer bladder with the sleeve wrapped around it. This form of a pneumatic actuator is very common and consists of a bladder generally made of latex or rubber while the sleeve is usually a nylon fibre as shown in Fig. 4.1. The braided sleeve makes initial angle with the horizontal axial axis of the actuator and this braid angle increases when the inner bladder expands. This increase in the braid angle compresses the entire muscle in an axial direction thus producing a linear pulling force. However, the braid angle is limited to a maximum of $54°44'$ after which the muscle will increase in

length and decrease in diameter. The compliance, high force-weight ratio as well as the lack of any metallic parts make the McKibben muscle highly desirable as a actuator in our design.

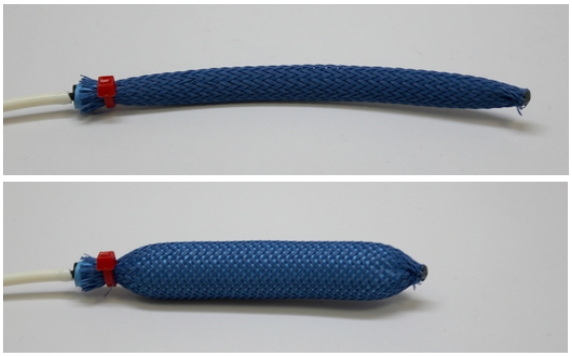

Figure 4.1: An example of a McKibben artificial muscle. From Roche (2019)

4.3 Parameters

The McKibben actuator patent was filed by Gaylord in 1955 as an orthopedic device. Its purpose was to replace the ordinary piston cylinder arrangements. Prior to fabricating the McKibben muscle we must find a suitable model, through which, a general idea of the parameters of the muscle can be determined. The model should be able to give us an understanding of the muscle parameters and give a rough estimate of the force produced by the muscle. Doumit et al. mentions different models for calculating the force generated by the muscles. In his paper he mentions that the models presented earlier by Ching-Ping Chou and Hannaford and Tondu and Lopez. He explains that Tondu and Lopez tried to improve the accuracy of the model presented as an ideal cylinder in Eq. 4.1 by including non-cylindrical terms:, However their parameters are estimated via experimental data. The also validate their model and conclude to have a low accuracy at low pressures. This therefore cannot be used to estimate the force of our muscle. The model derived by Ching-Ping Chou and Hannaford also includes non cylindrical terms but they have not validated their model nor have provided an accuracy of the results. Their model is based on comparing the parameters of the artificial muscles to human muscles. Doumit et al. tries to correct the force calculations with their own model; However, the model proposed is complicated as it requires the stress parameters of the sleeve and is not used in this case. Instead we use the model provided by Tondu of an *ideal* McKibben muscle which is shown in Eq. 4.1, given below.

$$F = \frac{\pi D_0^2}{4} P[a(1-\epsilon)^2 - b] \tag{4.1}$$

$$\text{with,} \quad a = 3/\tan^2\alpha_0, \quad b = 1/\sin^2\alpha_0 \text{ and } \quad \epsilon = \frac{l_0 - l}{l_0}$$

Where D_0 is the muscle diameter at rest, P is the pressure supplied, ϵ is the contraction ratio of the muscle i.e change in length per unit original length. α_0 is the initial angle the fibres make with the horizontal axis of the muscle. It can be seen from the equation that the force is a function of the input pressure as well as the contraction ratio ϵ. The expressions for maximum force and contraction ratio can be obtained at $\epsilon = 0$ and $F = 0$ conditions respectively.

$$\begin{cases} F_{max\,ideal} = \pi r_0^2 P(a-b), & at \quad \epsilon = 0 \\ \epsilon_{max\,ideal} = 1 - \frac{1}{\sqrt{3}\cos\alpha_0}, & at \quad F = 0 \end{cases}$$

4.3.1 Length

The length of the artificial muscle is the entire length of the core as well as its end tips. The active length of the muscle is the length of its core in a state of no pressure. As the muscle expands radially pushing on the braided sleeve the length of the muscle decreases upto a certain point which is restricted by the braid. Kothera et al. have shown that different length actuators in a blocked force setup do not affect the force measurements as increasing the length does not change the radial expansion or change the braid angle. Daerden and Lefeber have experimented with theses muscles in free contraction against a static load. They point out that in free contraction each of the load and pressure pairs has an equilibrium length.

4.3.2 Diameter

The *inner diameter* is the inner chamber in which air is pressurized for actuation. According to Ching-Ping Chou and Hannaford the force is proportional to the change volume per change in length. As the inner core can be assumed as a perfect cylinder we know that $V = \pi r^2 L$ hence, increasing the diameter would increase the capacity of pulling force the muscle can generate.

The *outer diameter* determines the thickness of the bladder. The greater the thickness of the muscle the more energy it can store as it requires more pressure to achieve contraction. Therefore, the larger the thickness the the less force is generated at the same pressure. This can be seen in the experiments performed by Kothera et al.. On the other side if we use a very thin bladder the amount of pressure it can sustain is much less and a too thin bladder would expand out through the sleeve.

4.3.3 Braid angle

The braided sleeve is responsible for controlling the expansion of the bladder. As the bladder expands the angle of the braid increases the angle will continue to increase until $54°44'$ as seen in Fig 4.2. Any further increase in the braid angle beyond this point the bladder would have to elongate and decrease its diameter (Tondu, 2012). This angle is validated through experiments and also if the force in the Eq. 4.1 is 0N we get the angle of the braid as $54°44'$. A lower initial braid angle would provide a larger working range.

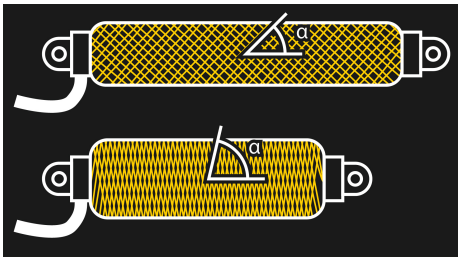

Figure 4.2: Increase of Braid angle on expansion. From Walter (2016)

4.4 Design

In this section we present the design of the artificial muscles also know as Pneumatic Artificial Muscle (PAM). We first give a brief description of the design to be molded, followed by the curing and fabrication of the silicon bladder. We then present the design limitations of the basic PAM design for higher load applications. To overcome the limitations of the basic PAM we design new end cap structures for supporting the basic structure of the bladder and braid.

4.4.1 Initial design

The design of our muscle was based on various sources such as Doumit et al. (2009), Kothera et al. (2009) and Tondu (2012). An existing braid of diameter 14mm was used as the basic para-

meter. Kothera et al. shows that a greater thickness of the silicon bladder allows for greater pulling force as compared to thinner bladders. Our actuators thickness was taken as 3mm. The length of the muscle is the length of the inner cylindrical chamber of the muscle which will expand when pressurized. To prevent any obstruction to the inflation of the inner core, extra silicon is added to the length of the muscle on each end. These are called tips, which provide a base for clamping/holding the braid onto the silicon bladder. They also provide support through which the muscle can transfer the force generated onto a surrounding mechanism. These tips are analogous to the tendons connecting human muscles to the bones. The length of the core was set to be 120mm with each tip being an extra 10mm for a total muscle length of 140mm A schematic of the silicon bladder is shown in fig 4.3

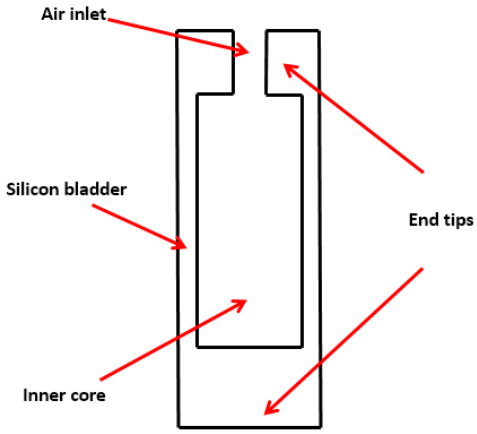

Figure 4.3: Schematic of the silicon bladder

A 3D printed mold was created into which we pour silicon (Ecoflex 00-50) which then cures to create our silicon bladder. Fig. 4.4 shows the mold created in SolidWorks. The part of the mold which gives shape to the inner core is attached to the end cap through a rod with threading on one end. These threads on the inner cavity of the cap and the rod were machined as the core with the rod had to aligned perfectly straight to avoid a bladder with varying thicknesses. This would result in an uneven bladder expansion. The rod also allows to create a passage for the pneumatic pipe into the main bladder core. The diameter of the rod was taken accordingly. The modularity of the mold was also taken into consideration where for a constant length the inner core can be switched easily to allow easy changes in the muscle design. To avoid air gaps in the mold from deforming the required structure the silicon was poured into the mold from a hole located on the lower end of one of the shells. Few air hole were also created in the top cap. This allowed the silicon to fill evenly throughout the mold from the bottom while air is able to escape through the holes in the top cap.

4.4.2 Design limitations

There were two major design limitations of the standard PAM model, which restricted its use in higher force applications and as such must be addressed.

Deformation at end tips: Plastic toothed clamps were used to clamp the braid tightly onto the bladder; However, the deformations caused by the ends of the inner core caused an axial outward force on the clamps which would push the clamps off its ends. This would also break away the ends of the braid and opens the weave. As a result the muscle would break on contraction even under no load conditions.

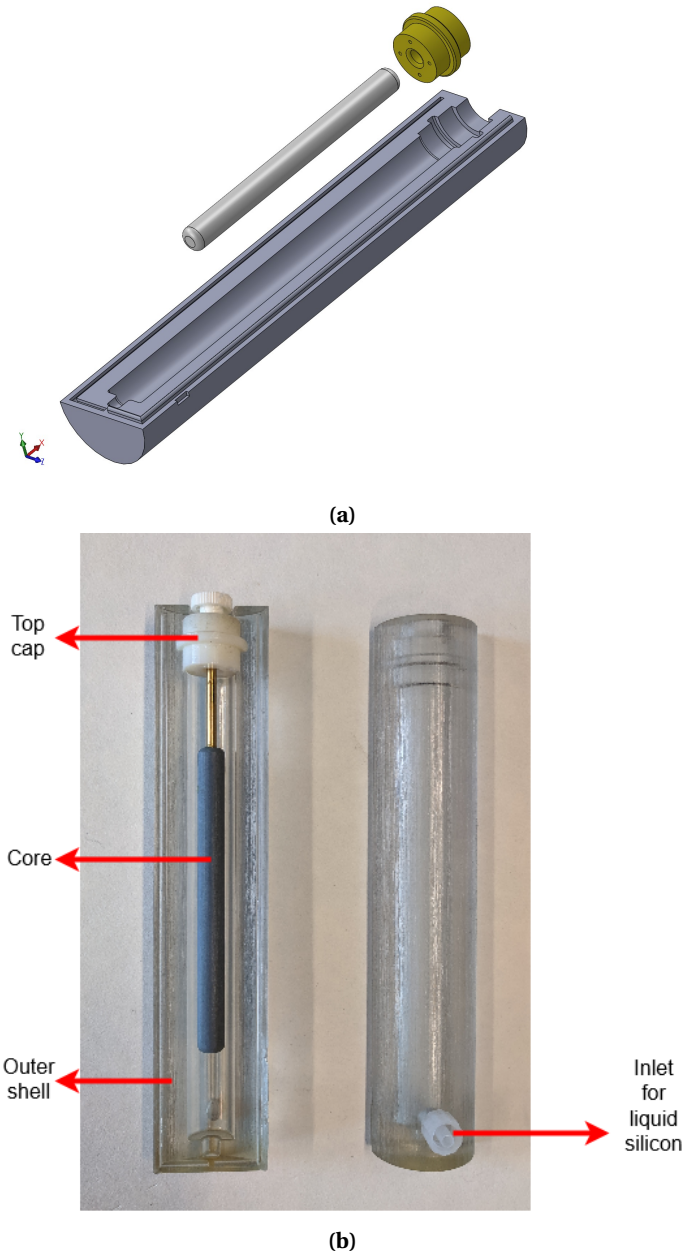

Figure 4.4: 3D printed mold for silicon based pneumatic McKibben muscle. a) The 3D designed CAD model of the mold. b) Fabricated mold.

To avoid this the tip length was increased to 25mm on each end. The shell used in the previous mold was reused with the exception of the inner core. The length of the core was reduced to 90mm to accommodate the tips. This solved the problem of the end clamps breaking off in a no load condition and the muscle is able to freely contract upto a pressure of 2 Bars.

Muscle contraction under loading: We have solved the issue of the clamps breaking off due to forces of the muscle core on the tips. The other problem arises when a load it attached to the end of the artificial muscle. The external loads produce an axial force which causes the clamps to slip off the open ends of the muscle shown in fig 4.6. To prevent the clamps from sipping off we design new end caps which are to be placed at the end tips of the bladder.

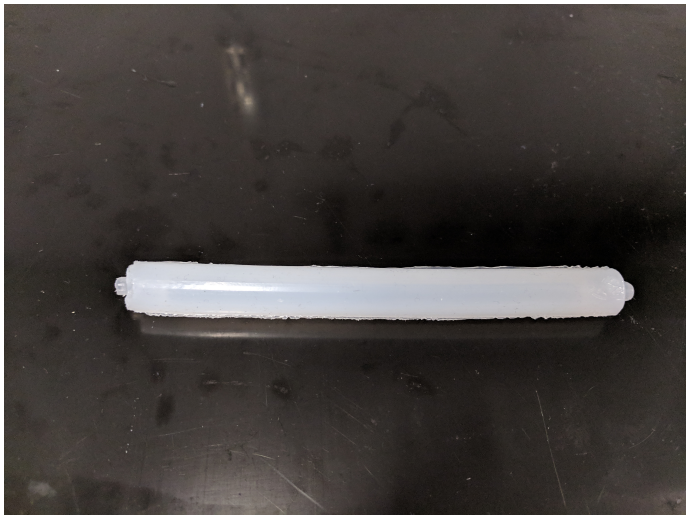

Figure 4.5: Silicon bladder after removal from the mold.

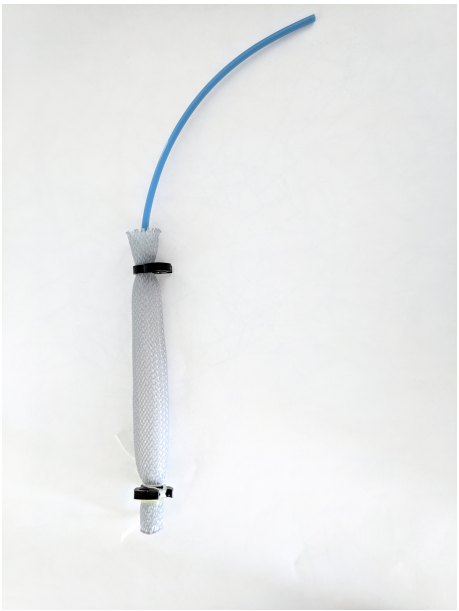

Figure 4.6: Fabricated basic Pneumatic Artificial muscle.

4.4.3 Modified design for higher force application

The clamps breaking off is due to the axial force exerted by the muscle is far greater than the friction between the braid and the clamp. To overcome this issue Mori et al. describes their design to instead use a base ring structure. The braid is to be wrapped over and around the ring and then clamped onto the muscle. These rings are the supports through which the muscle can transfer its force. The reversing of the braid over the ring prevents further slipping of the braid. The ring mentioned by Mori et al. is attached to the metallic intake tube of the muscle which has a groove to lock the ring in place.

A similar structure was designed with a few modifications. The parts were 3D printed rather than using metallic parts. The ring like structure is not attached to the nozzle, rather its pulled over the initial braid over the ring structure. The braided sleeve is then wrapped backwards over the ring and is then clamped. A cap is also designed which is to hold the ring in place and to provide an outer shell, which can then be used to connect the muscle to external fixtures.

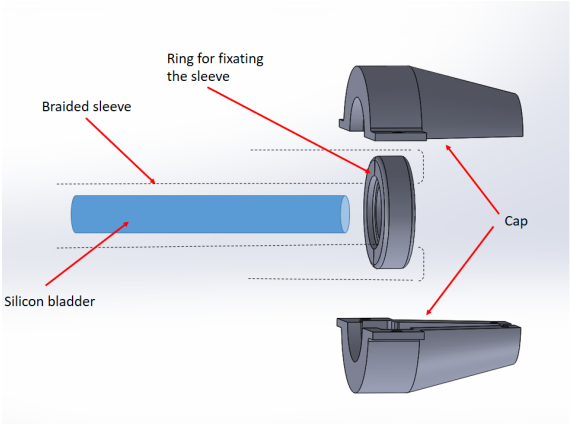

Figure 4.7: Visual representation of assembling the artificial muscle.

Fig 4.7 shows a visual representation of the wrapping of the braid. Addition of these end caps have also increased the overall length of our muscle to 210mm.

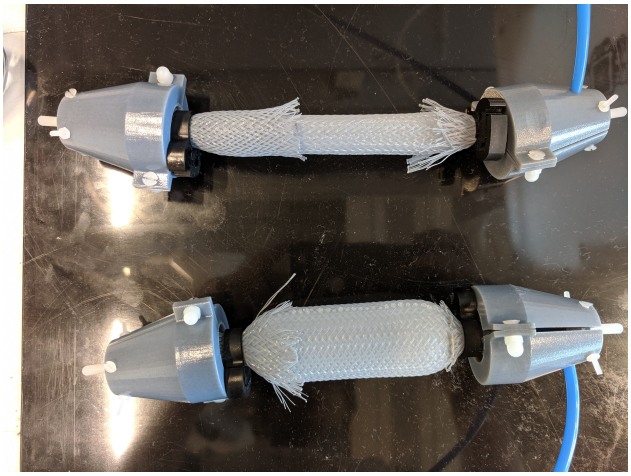

Figure 4.8: Fabricated muscle in unactuated and actuated conditions.

4.5 PAM force characterization

Once the muscle was fabricated it was needed to find the correlation between the pressure input to the muscle and the force the muscle is able to transmit. The force of a McKibben muscle varies between different applications and different models used by each researcher. Tondu states that the muscle produces its maximum force at full extended configuration with just enough pressure for the bladder to start expansion but not produce significant deformation yet. The full contracted configuration the muscle is said to produce 0 force. This is in accordance with Eq. 4.1 when the contraction ratio ϵ is at its maximum. Doumit et al. mention using a tensile testing machine to measure the force, where they also using a similar model came to the conclusion that the muscle force decreases as the muscle length decreases. Kothera et al. also mentions using a dynamic and fatigue testing machine but they kept the pressure constant and performed a slow load ramp till force measurement reached zero. Mori et al. use their hydraulic muscle to apply pressure onto a hydraulic piston whose pressure is then calculated to find the force of the muscle. In all the above methods of measuring the force generated by the muscles is based on their contraction ratio. Pressure is increased to reach a certain contraction ratio and the force is measured at that point.

The force characterization of a McKibben muscle varies depending on the model used by researchers. Most of the literature on McKibben muscle are either review papers for different types of actuators or are based on fabrication of the muscles and their braids as a verification for different static and dynamic models. Very little is information is available on these muscles being used as an actuator for a particular application. It is true that since these actuators resemble human muscles and are often compared as such. Human muscles are said to have zero force when contracted and as such models of McKibben muscles follow the same concept (Daerden and Lefeber, 2002).

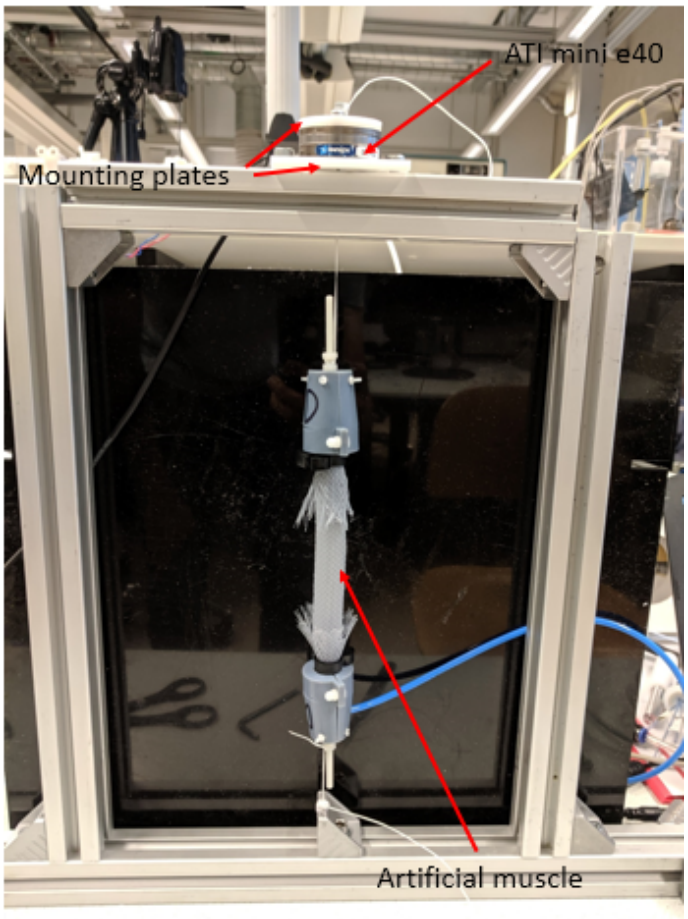

Figure 4.9: Force characterization test setup.

4.5.1 PAM force characterization test setup

The purpose of using a McKibben muscle in our case is to assist the hamstring muscle group and to prevent ATT. To characterize the force for this configuration a setup was created as shown in Fig 4.9 to be able to measure the blocked-pulling force and an ATI mini-e40 six-axis force torque sensor was used to calculate the pulling force of the muscle shown in Fig 4.10. The functional block diagram of the test setup shown in Fig. 4.11 This setup allows us to measure the force as a function of pressure. One end of the muscle is attached to the base of the setup while the other end is connected to the mounting plate above the force sensor. On contraction the muscle will pull the mounting plate applying force to the sensor which is then recorded against the pressure input. The pressure is controlled by a FESTO 2 bar pressure regulator (veab-l-26-d2-q4-v1-1r1) through an arduino UNO micro-controller board. A Matlab app is used for controlling the regulators through a GUI. Once the relation is established, we use interpolation to provide the pressure control value to the arduino for user entered force requirements of the muscle.

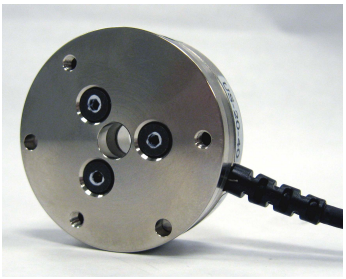

Figure 4.10: ATI mini-e40 force torque sensor

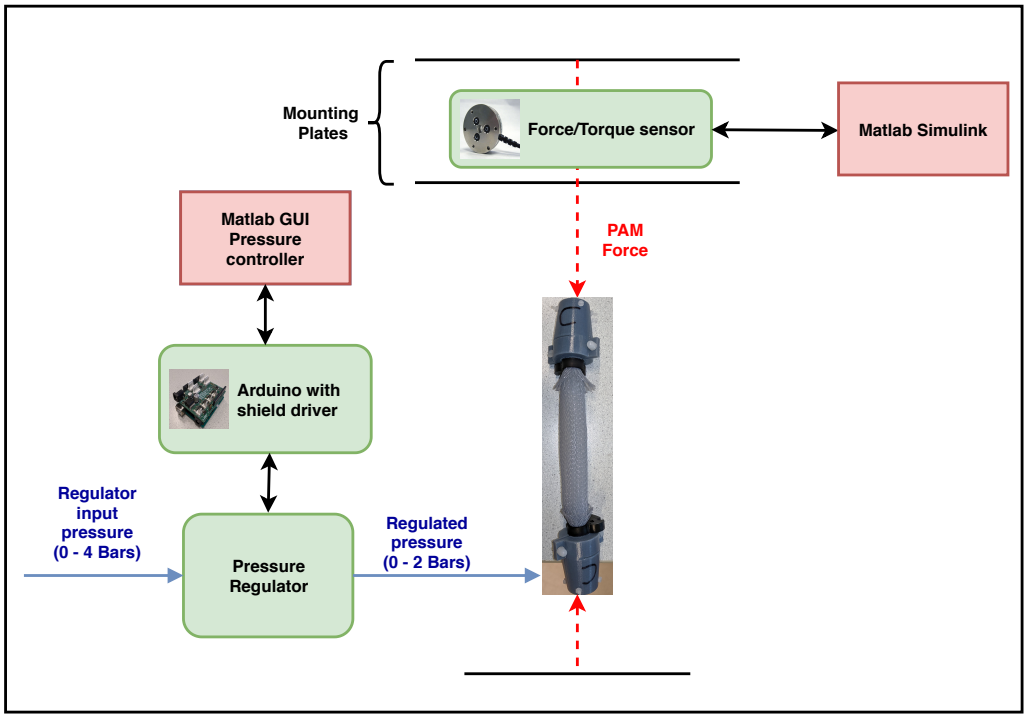

Figure 4.11: Functional block diagram for PAM force characterization.

4.6 PAM characterization results

A total of four muscles were fabricated with the new cap design and each of them were characterized separately. Each of the muscles were able to withstand 2 bars of pressure without any damages to the muscle itself. The muscles are able to produce forces around 50N. The characterization curves for the muscles can be seen in Fig 4.13. The contraction ratio of the muscles was observed to be around 12% of the original length of the muscle including the end caps. Interpolation of the force characterization graphs were then used in a Matlab App to estimate the pressure required by each muscle to produce the required amount of force the Matlab GUI can be seen in Fig 4.12.

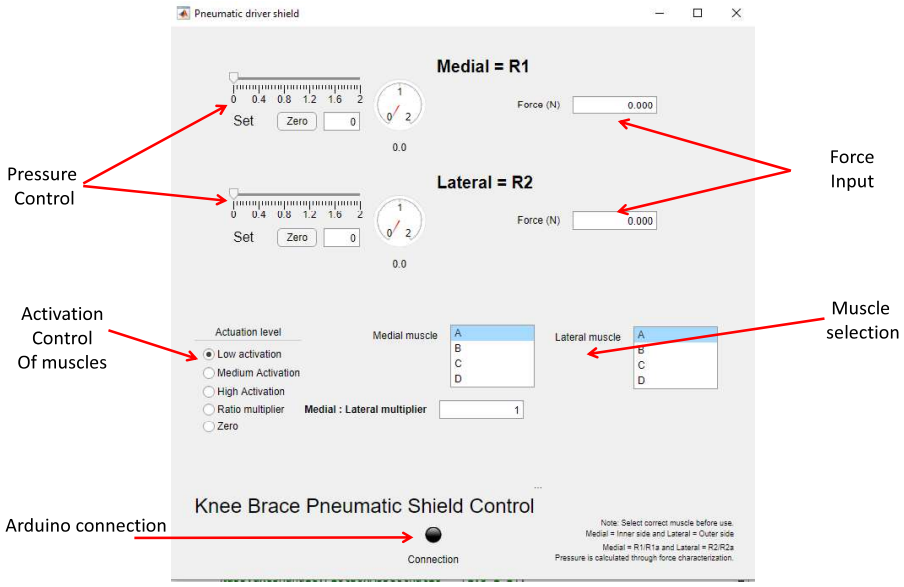

Figure 4.12: Matlab app used for controlling the artificial muscles.

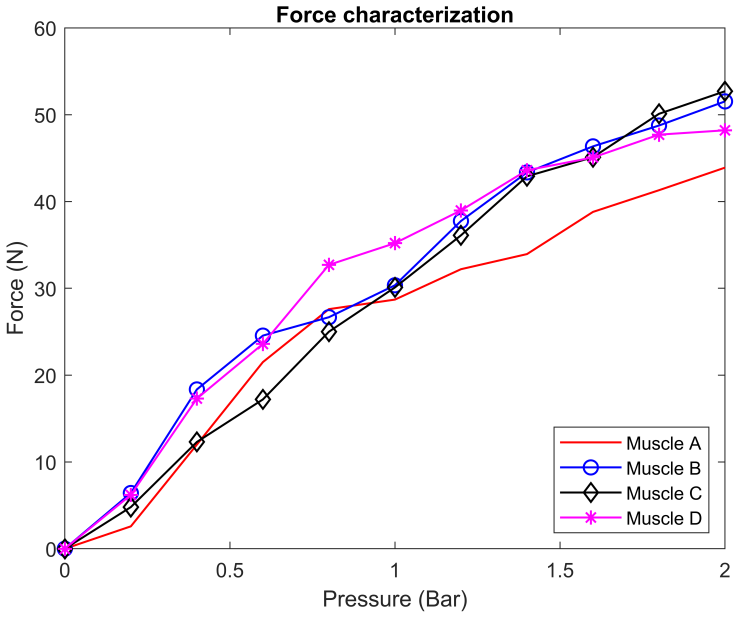

Figure 4.13: Force characterization graphs for the fabricated PAMs.

5 Knee brace integration

In this chapter we discuss the integration of our PAMs onto a knee brace with the goal of assisting the hamstring muscle group. By assisting the hamstring muscle group we try to regain the stability lost by an ACLD knee. We first discuss the type of brace used and the supporting structures required to transmit the actuation of our PAMs onto the knee joint. An available knee brace was used and changes were made to the brace according to our requirements. We add two support structures to the brace one for the femur and one for the tibia.

5.1 Design

To be able to design our soft robotic knee brace, an available knee brace (From physioroom, UK) was used as seen in Fig. 5.1. This brace is used as a base on which we mount external support structures which will direct the forces onto the anterior of the tibia. The knee brace used as the base was a common hinged knee brace from PhysioRoom. A hinged brace was chosen as it provided necessary support to the brace and also prevents the brace from axially contracting. Three main support structures were designed and are explained below.

Figure 5.1: The available knee brace used as the base of our design.

5.1.1 Hinges

The existing hinges from the knee brace were required for the proper movement of the brace with the knee. This was to avoid the brace from wrinkling on flexion of the knee. The hinge consists of two flat plates, one of which is kept parallel to the thigh and the other one parallel to the tibia. A double spur gear mechanism is applied to these plates to mimic the movement of the synovial knee joint: However, the hinge is made of metal and is not suitable for any MRI experiments and as a personal observation the hinge seemed to be too tight and as a result the motion was full of small incremental jerks. This is highly undesirable which is why they were replaced with a plastic hinge of similar dimensions as shown in Fig. 5.2.

The spur gears of the system were modified according to ISO standards and the parameters can be seen in table 5.1

The gear ratio of the hinges is 2 instead of 1 even though both gears are the same. This is because when the hinges are placed in the brace the plates parallel to the femur is considered fixed. While the gear connected to the tibia is said to rotate around the first gear similar to the

Table 5.1: Spur Gear parameters

Gear ratio	2
Module	1
Internal Diameter	21.5mm
External Diameter	26mm
Primitive diameter	24mm
No. of teeth	24
Pressure angle	20°

working of a planetary gear. In which case the gear ratio is given by

$$\tau = \frac{z_1 + z_2}{z_1} \tag{5.1}$$

Where, z_1 is the number of teeth of the gear connected to the femur (sun gear) and z_2 is the number of teeth of the gear connected to the tibia (driven gear). AS the number of teeth are the same the gear ratio is 2. The gear ratio is calculated even though there is no premise in our current design of using the hinges to evaluate any parameter of our knee brace; However, it maybe required to measure the angle of the knee joint. In such a case the gear ratio will be required if the hinge movement is used to evaluate the knee flexion angle.

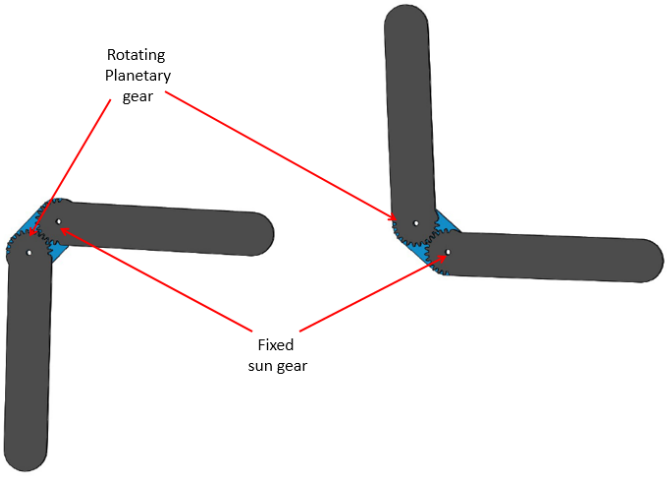

Figure 5.2: Gear interaction of hinges as a planetary gear system.

5.1.2 Femur support

The femur support structure has a requirement to be firmly attached to the femur. This is to allow maximum force to be transmitted to the tibia. Using this support structure as an anchor for transmitting the force it needs to be attached rigidly to the femur. This is done by attaching the structure to one of the arms of the hinges.

The support itself is laser cut from a 3mm thick Polyoxymethylene (POM) material. Grooves of 0.25mm thick and 1.5mm deep were cut. These grooves are required to be able to bend the flat plate into a U - shape. A semicircular cut was made to accommodate the lower leg in flexion. Fig. 5.3 shows the sketch used to laser-cut the POM material.

5.1.3 Tibia Support

The tibia support is a a curved 3D printed part which covers the anterior part of the tibia as shown in fig 5.4. This structure allows for directing the force in a posterior direction with the

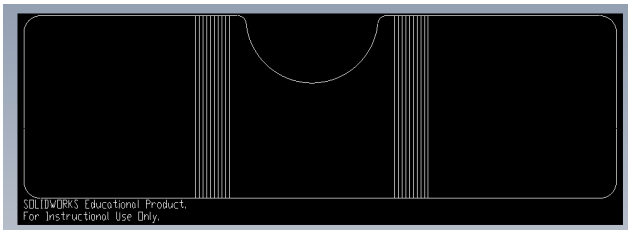

(a)

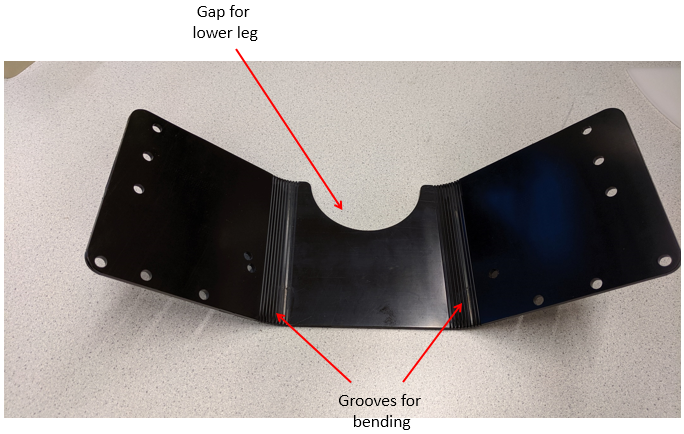

(b)

Figure 5.3: The laser cut Femur support. a) Sketch to cut the support. b) Final support plate bent using the cut grooves.

aim of decreasing the ATT motion of the ACL ruptured knee. The structure is made to cover the entire lower section of the brace, rather than a thin plate to widen the area of effect. The support is not made thin as this would increase the pressure concentration at that point and would lead to discomfort or the patient may experience a sharp pain when actuating the brace. This support is attached to the brace using velcro straps sewed onto the brace.

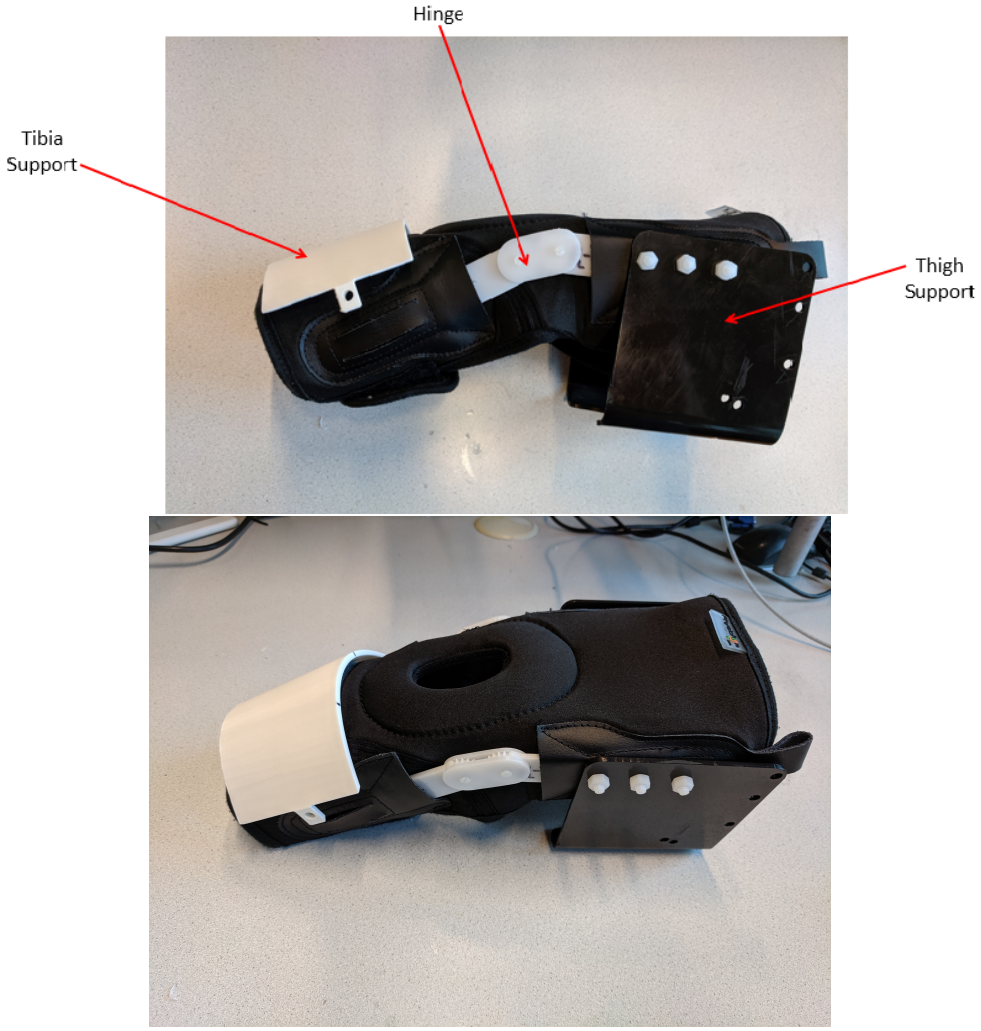

Figure 5.4: Integration of the support structures onto the knee brace.

5.2 System integration

The metallic hinges were replaced by our new hinges. The femur support is attached to the hinges after being bent. The size of the thigh may vary among individuals, thus the bending of the femur support allows for compliance in being able to attach the femur support to the hinges. Further we attach the tibia support to the anterior of the tibia. Connectors were made to attach the PAMs to the support structures. The integration of the support structures on the knee brace can be seen in Fig. 5.4.

The fabricated PAMs are to be implemented on our knee brace. We do not propose a fully dynamic knee brace for the full range of knee flexion. The artificial muscles produce force on contraction and have a limited contraction ratio of 12% and are to be attached to the thigh support as well as the tibia support. However, during flexion the distance between the two supports plates continues to decrease beyond the minimum length of the actuated PAMs. As a result one point of attachment is not sufficient for the entire range of motion. The PAMs are therefore, attached for selected angles of flexion at 0°, 30°, 45° and 60°. The attachment sites are such that the PAMs are stretched in each of the chosen flexion angles, so as to apply the forces estimated from the characterization curves effectively to reduce the anterior motion of the tibia. An illustration is presented in Fig. 5.5 of the different attachment sites for the PAMs.

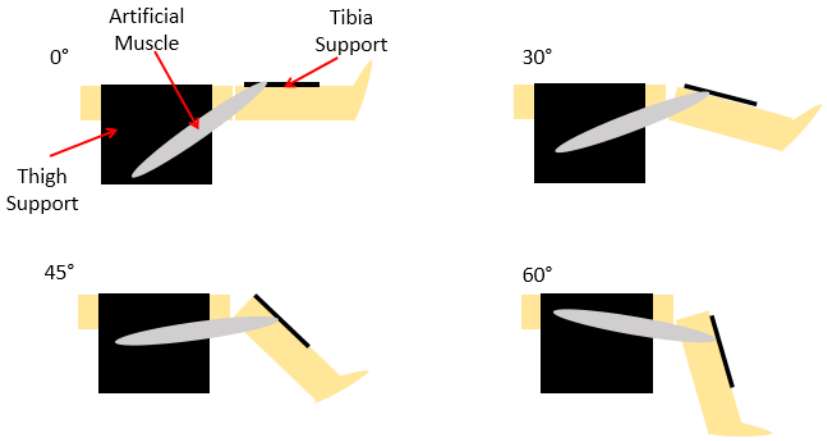

Figure 5.5: Illustration of the attachment sites for the PAM in different angles of knee flexion.

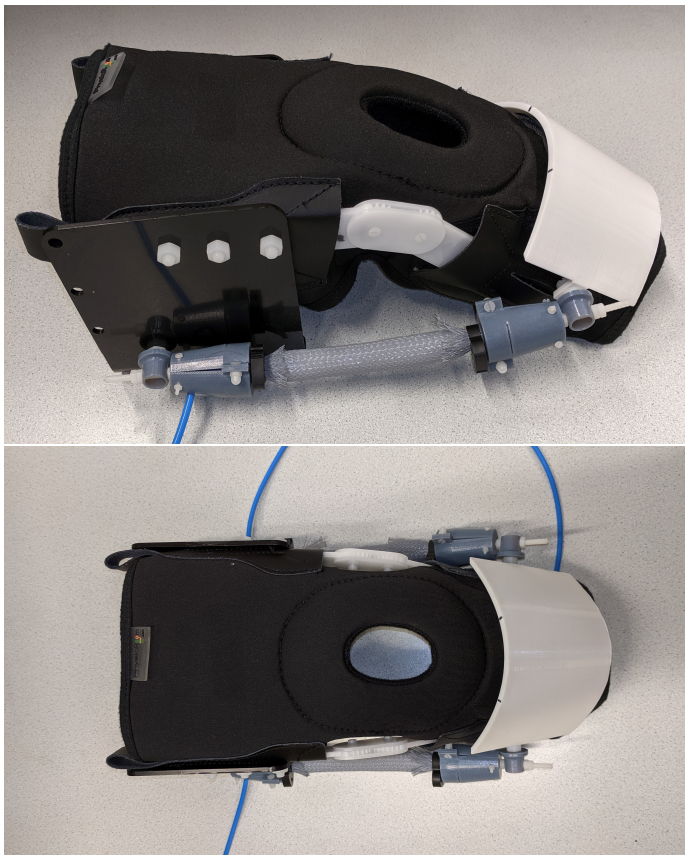

Figure 5.6: Integration of the PAMs onto the knee brace in the 0° configuration.

6 Evaluation of the Knee Brace

6.1 Purpose

Before the brace is tested on ACL rupture patients, we first test the feasability of our brace on participants with intact ACLs. We present two experiments to validate our results, one being a surface Electromyography (sEMG) test and the other being a laxity test to prove a reduction of the ATT motion. The sEMG experiments consisted of measuring the activity of the hamstrings in a static and dynamic condition. Since the hamstring activation is said to reduce the instability of the knee present in an ACL deficient knee Li et al. (1999); Liu and Maitland (2000), we aim at assisting the hamstring muscles in knee flexion. The laxity experiment is out of the scope of this thesis but, we believe it is a crucial method for evaluating the effect of our brace. As such we present a porto knee testing device, which is a clinical device used to check the laxity of an ACL or PCL ruptured knee.

6.2 Activation of the knee brace

Prior to preforming the experiments we must first select the appropriate forces applied by the brace onto the joint. The knee brace contains two PAM's, one for the medial side of the knee and the other being for the lateral side of the knee. We elaborate on two types of actuation for the knee brace based on the force's produced by the individual PAM's.

6.2.1 Symmetric actuation

In this case both the PAM's apply the same amount of force on each sides. We apply three different levels of symmetrical actuation to our brace to see the effect in reducing overall hamstring muscle activation in participants with an intact ACL. The different activation levels of the muscles are as follows:

- *No activation level:* In this case the brace is unactuated and the force produced by the PAMs is 0N.
- *Low activation level:* In the case of low activation the brace is actuated with each PAM generating forces of 10N.
- *Medium activation level:* This level increases the force generated by the PAMs to 20N each.
- *High activation level:* In this case the PAMs generate forces of 25N each. The PAMs are capable of generating much higher forces; However, keeping safety of the wear in mind the force is limited to not harm the participants leg.

6.2.2 Asymmetrical actuation

The flexion of the knee is not just a 2-D movement, the tibia also rotates around it long axis during flexion. This rotation of the leg is termed as the screw home motion of the knee and as such the PAM's should be actuated differently and not just with equal forces. The Fig. 6.1 shows the rotation of the tibia along the long axis during flexion/extension.

We use a validated finite element model of the knee to evaluate the forces required on each side of a ACLD knee to regain the stability lost due to the rupture of the ACL while, an anterior force of 100N was applied to the tibia in different flexion angles. A ligament continuum finite element model form Naghibi Beidokhti et al.,2017 was used to optimize the forces. This model contains the tension and strain values from the ligaments present in the knee. The ACL was

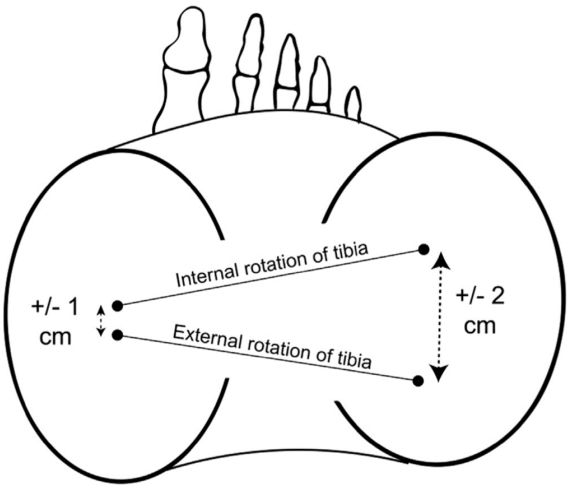

Figure 6.1: Depiction of the rotation of the tibia along its long axis during flexion/extension. The points represent the point of contact of the tibia and femur. From Aweid et al.,2019

severed in the model and simulations were run to optimize the forces required by the PAMs acting on the knee to regain the stability lost by the removal of the ACL.

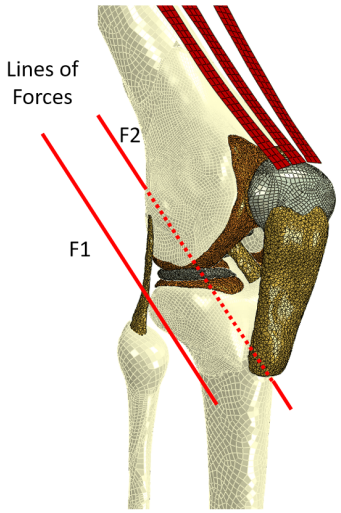

Figure 6.2: Finite element model of the knee used to evaluate the forces required to regain stability of the injured knee. From Naghibi Beidokhti et al.,2017

Through simulations it was found that a medial force of 14.5N and a lateral force of 3.8N is required to regain the lost stability in the finite element model when the ACL is severed. The image of the finite element model can be seen in Fig. 6.2. We express the medial and lateral forces as a *ratio setting* where the medial:lateral forces are 14.5:3.8N for the entire range of flexion of the knee.

The Table. 6.1 shows the forces on each side of the knee for each activation level discussed above.

6.3 Experiments for knee brace evaluation

In this section we present two methods of evaluation of our brace. The first one being the surface Electromyography (sEMG) test, where we measure the electrical activity of the hamstring muscle group. The sEMG experiments are caried out during a static exercise known as the

Table 6.1: Forces applied by the brace for different levels of PAM activation

PAM Activation setting	Medial(inner) Force	Lateral(outer) Force
No Activation	0N	0N
Low Activation	10N	10N
Medium Activation	20N	20N
High Activation	25N	25N
Ratio setting	14.5N	3.8N

seated hamstring curl and during an active/dynamic exercise which is normal walking (gait). The laxity test presents a device known as the porto knee testing device (PKTD) to asses the laxity of an ACL ruptured knee. The laxity test though not a part of this thesis, can yet be an effective method of evaluating the strain on the soft tissues present around the knee.

6.3.1 Surface Electromyography

Surface Electromyography has been used extensively for measuring the activity of various muscles. This method utilizes the small electrodes placed on the surface of the skin directly over the targeted muscle. The electrical activity of the active motor unit is then measured. The signal from the electrodes is amplified using an amplifier (Micromed MATRIX Light). Raw EMG data from the amplifier is then processed using the systemPLUS evolution software by Micromed to record and visualize the EMG signals. The amplifier has two channels and two pairs of electrodes that can be used simultaneously to acquire two signals.

Placement of electrodes

The hamstring muscle group consists of three muscles namely the Semitendinosus (ST), Semimembranosus (SM) and the Bicep femoris (BF) and can be seen in Fig. 6.3. The hamstring have two major functions: one being the ability to extend the hip joint and the other being the flexion of the knee joint. The ST and BF (long head) are located just below the skin and are the most superficial muscles of the hamstring group, which is why the electrodes are to be placed on the belly of these muscles. Crosstalk signals are distortions generated in the sensors due to electrical interference from neighboring muscles around the targeted muscle. To avoid crosstalk the spacing between the electrodes is kept at 10mm for each pair of electrodes De Luca et al., 2012.

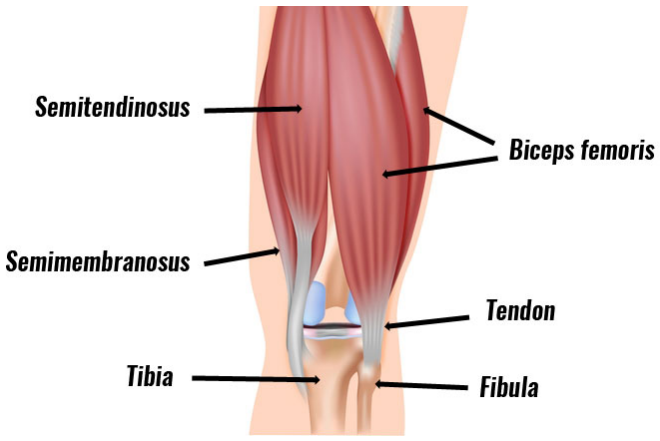

Figure 6.3: Anatomy of hamstring muscle group of the right leg. From Walden

The electrodes will first be slightly made wet by salt water and then placed on the skin of the patient. An earth electrode connected to a strap is placed around the wrist. It is used to reduce

any unwanted noise signals. One pair of electrode will be attached over the ST and the other will be placed over the BF. The electrodes used were Al/AgCl circular sensors.

EMG Experiment

In our study we perform the EMG test in two cases: a static case and in a dynamic case. In the static case the leg is placed under physical stress such that the hamstrings are activated, in our case we place the leg in a seated hamstring curl position. Whereas in the dynamic test we measure the activation of the hamstrings during walking. The hamstring activation is then compared with the readings from a non-actuated brace condition for different activation levels of the pneumatic muscles for both cases.

Static test: The EMG data is acquired during a seated hamstring curl exercise using a resistance band as shown in fig 6.4. The resistance band is attached to one end of a rigid support such as a table. While the leg is place inside the band at the other end. The resistance band is stretched such that it produces an anterior force of 50N on the tibia. The participants were then asked to keep the leg stationary during the experiment. We perform this exercise with the knee at 60° and the hips reclined back at an angle of 110°. This angle of the knee and hips ensure a maximum activation of the hamstrings in the whole range of motion of the exercise (Halaki and Ginn, 2012). Following this the maximum voluntary isometric contraction (MVIC) is preformed to obtain the maximum activation of the muscle. This data is then used to normalize the following EMG signals from the experiment. All further signals are hence normalized as a factor of the maximum activation. Since EMG amplitude cannot be compared without a reference this maximum activation gives us a range for comparing the activation of the hamstrings before and after the activation of our artificial muscles. A detailed protocol of the experiment is given in Appx. A.

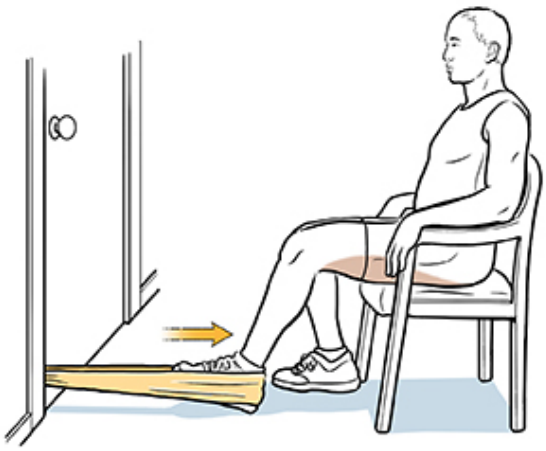

Figure 6.4: Illustration of a seated hamstring curl using a resistance band. From Fairview

Gait analysis: The designed knee brace should also be able to reduce the hamstring activation during daily activities. Thus, it suits us to study the efficacy of our brace during a gait cycle. To acquire the normalization factor we asks the participants to walk on the treadmill at a faster pace than normal. The remainder of the experiment is performed with the treadmill at a speed the participant feels matches their normal walking pace. EMG signals are taken for the gait cycle for different activation levels of the PAMs. A detailed explanation is mentioned in Appx. A.

Figure 6.5: Illustration of the gait experiment performed while wearing the knee brace.

6.3.2 Laxity test

The porto knee testing device (PKTD) is a device to measure the anterior, posterior and rotational instability of the knee joint using an MRI scanner (Espregueira-Mendes et al., 2012) and can be seen in Fig. 6.8. The device is used to generate an anterior motion of the tibia along the femur at different angles of knee flexion. Before we start our experiment with the device we must first look into clinical practices used to measure knee laxity, such as a Lachman test. The Lachman test consists of manually applying a force with the knee flexed at 20° to 30° and producing an anterior motion of the tibia as seen in Fig. 6.6. This angle of knee flexion produces the most anterior movement of the tibia along the femur (Logan et al., 2004). Although the test is performed by clinicians manually, a device known as the KT1000 arthrometer (MEDmetric Corporation, San Diego, California, USA) is used to objectively evaluate the forces and laxity of the knee.

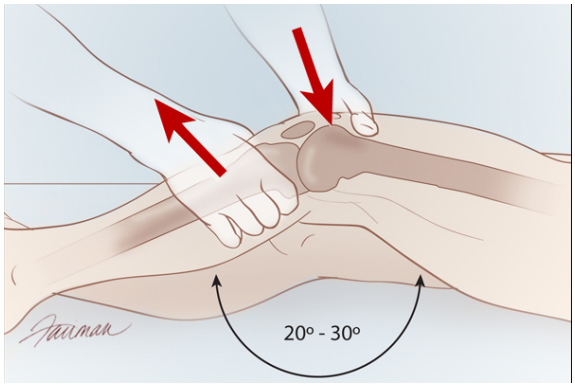

Figure 6.6: Illustration of a Lachman knee laxity test for ACL rupture. From Advisor

The PKTD device used is similar to the working of the KT1000, with the exception that the PKTD contains supports for fixing the knee joint angle. The piston present in the PKTD is shown in Fig. 6.8. Arneja and Leith, 2009 mentions in their paper the standard forces applied by the KT-1000 as being 67N, 89N and 133N. The 133N force produces the most anterior translation during the Lachman test at 30° of knee flexion. However, since the initial tests are performed on participants with an intact ACL it is not recommended to apply the maximum load of 133N instead application of a 89N load to the tibia should not damage the intact ACL. At 30° of knee flexion the ACL is tensioned (Rachmat et al., 2016) in patients with no ACL injury. In such a case the anterior displacement would be greatly affected, which is why we believe, it might be better to perform the experiment at 45° of flexion as the slack in the ACL would provide for more visible anterior motion without damaging or affecting the intact ligament.

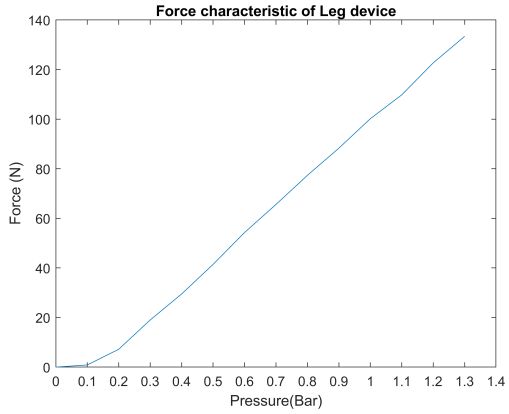

Figure 6.7: The force characterization graph for the porto-knee testing device.

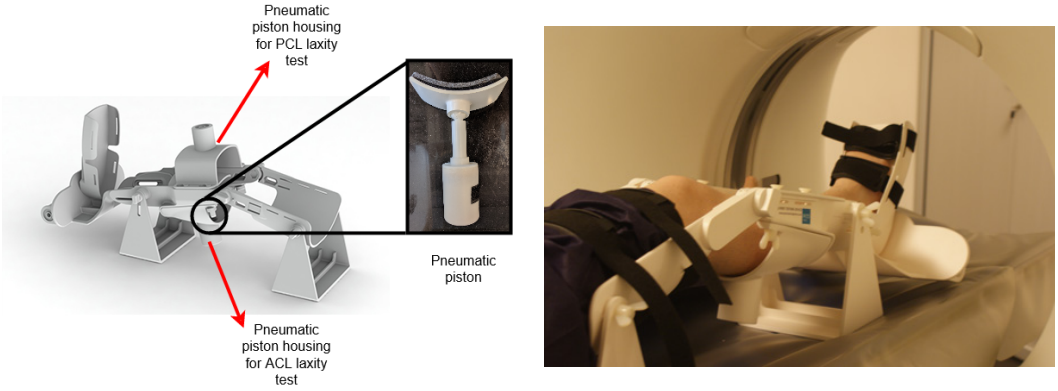

Figure 6.8: Porto Knee testing Device. Adapted From Espregueira-Mendes

Proposed Experiment

In this study as we aim to reduce the anterior movement of the tibia without affecting the underlying cartilage. As a result we propose to use the PKTD device to produce the anterior shift in the tibia while trying to reduce this shift using our brace. The test should be verified using MRI scans of before and after the activation of the brace. Prior to testing the efficacy of our brace, it will be required to determine the pressure required by the pneumatic piston of the PKTD to produce the required force . The pneumatic piston is characterized using the ATI mini e-40 force sensor and the graph of the force generated to the pressure supplied to the piston is given in Fig. 6.7.

The participants should then be asked to wear the brace and place their leg in the PKTD setting the knee flexion angle at 45°. The leg should then be inserted into the MRI scanner and images of the normal knee should be taken as a reference. A load of 89N is then applied to the posterior of the tibia creating a displacement. MRI scans are taken and then the brace is activated for the different levels of actuation. The MRI images should then be segmented.

7 Results and Discussion

In this chapter we present the results of the experiments presented in Ch. 6. We first present the results of the sEMG method of evaluation followed by a brief discussion on the results of the experiments.

7.1 EMG results

The EMG experiments were performed on 4 participants and their consent was taken prior to experiments. We first need to process the raw EMG data by filtering, rectifying and smoothing the signal. After the raw EMG data is processed, the hamstring activation during different levels of activation of our PAMs is compared to the hamstring activation level when the PAMs are unactuated.

7.1.1 EMG Processing

Raw EMG signals are inherently noisy and contain artifacts related to motion of the electrodes on the skin and the muscles below. External sources such as laptops and mobile phones may also introduce high frequency noises in the system. As a result it is common practice to first filter the noise from the EMG signal. EMG signals are generally in the range of 10/20Hz - 450/500Hz (De Luca et al., 2010), which is why we first filter the raw EMG signal with a band pass filter with cut off frequencies of 20Hz and 500Hz respectively. EMG signals are bipolar and have both positive and negative values in the same range. Thus EMG signals have a mean value very close to 0. The signals are therefore full wave rectified.

EMG signals related to muscle activation values do not make sense unless they have a reference value to be compared with Halaki and Ginn,2012. It is general practice to perform a maximum voluntary isometric contraction (MVIC), where the participant is asked to tighten the muscle under examination without contracting or expanding the muscle. This MVIC signal is used to normalize the following EMG signals using the RMS value of the MVIC signal. This normalization allows the muscle activation to be a percentage of the total activation possible by the individual. Finally, a moving average filter is applied to the normalized EMG signals. The Fig. 7.1 shows the EMG filtering process.

The MVIC is a good measure for normalizing static conditions such as the seated hamstring curl experiment; However, the MVIC signal does not produce good normalization results during dynamic activities. The change in the joint angle and the length of the muscles effects the EMG levels of the muscles and the MVIC is not a good template for normalizing EMG signals during dynamic motion. The book published by Halaki and Ginn mentions that a maximum isokinetic contraction of the movement under examination would be a good template for normalizing dynamic movement. In the EMG experiment for gait analysis the participants were asked to walk at a faster pace to obtain the normalizing signal. The maximum peak of the fast paced walk is used to normalize the EMG signals during the gait analysis experiment.

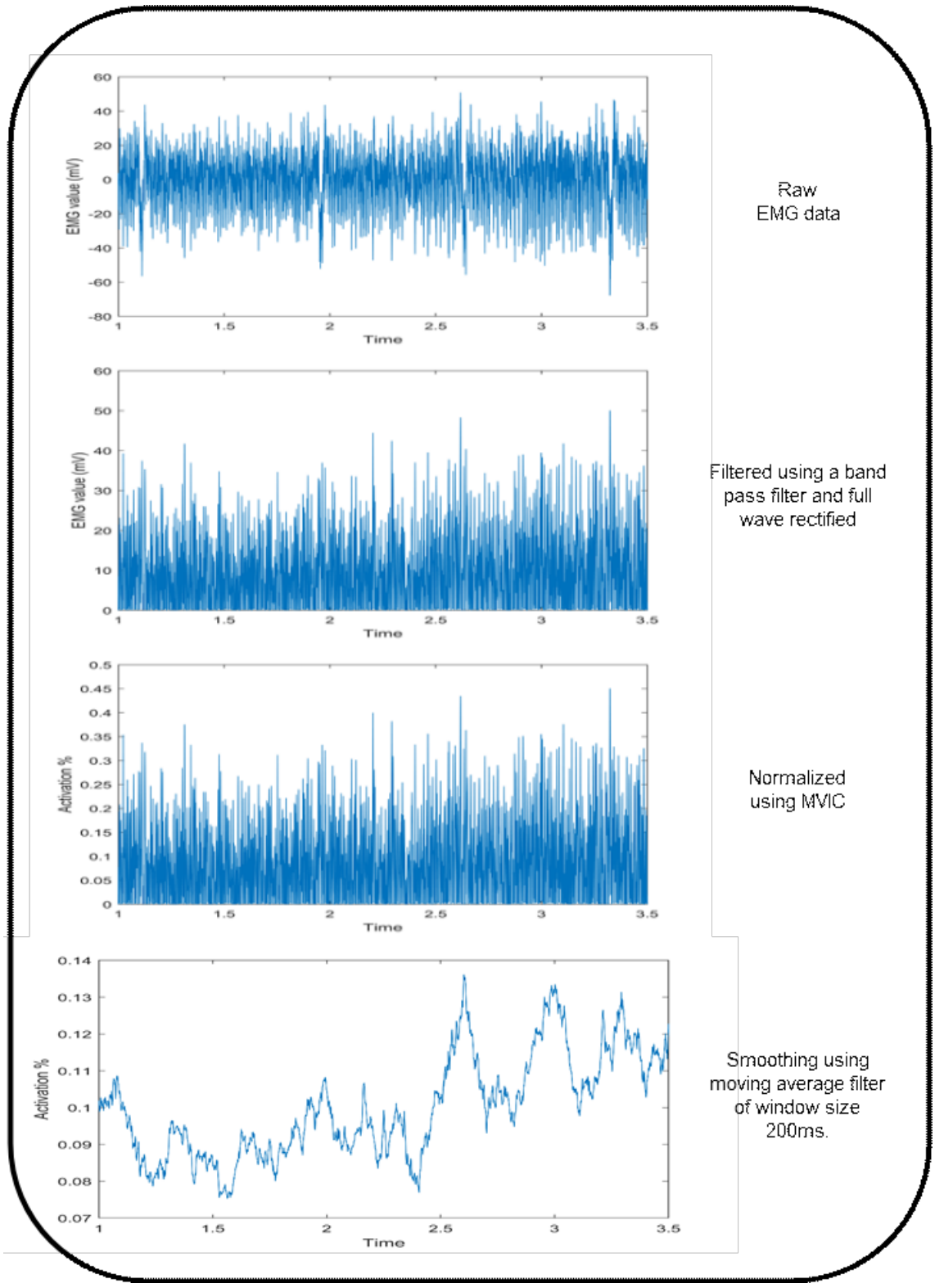

Figure 7.1: An example of the filtering process of the raw EMG data.

7.1.2 Static EMG test

The processed EMG signal from the seated curl experiment during the different activation level of PAMs is compared to the EMG signal when the PAMs are unactuated. The Fig. 7.2 show the activation level of the hamstring muscle group when the brace is unactuated and during different actuation of the PAMs. The mean reduction was calculated and are presented with their standard deviation for both of the recorded muscles in Fig. 7.3.

Results

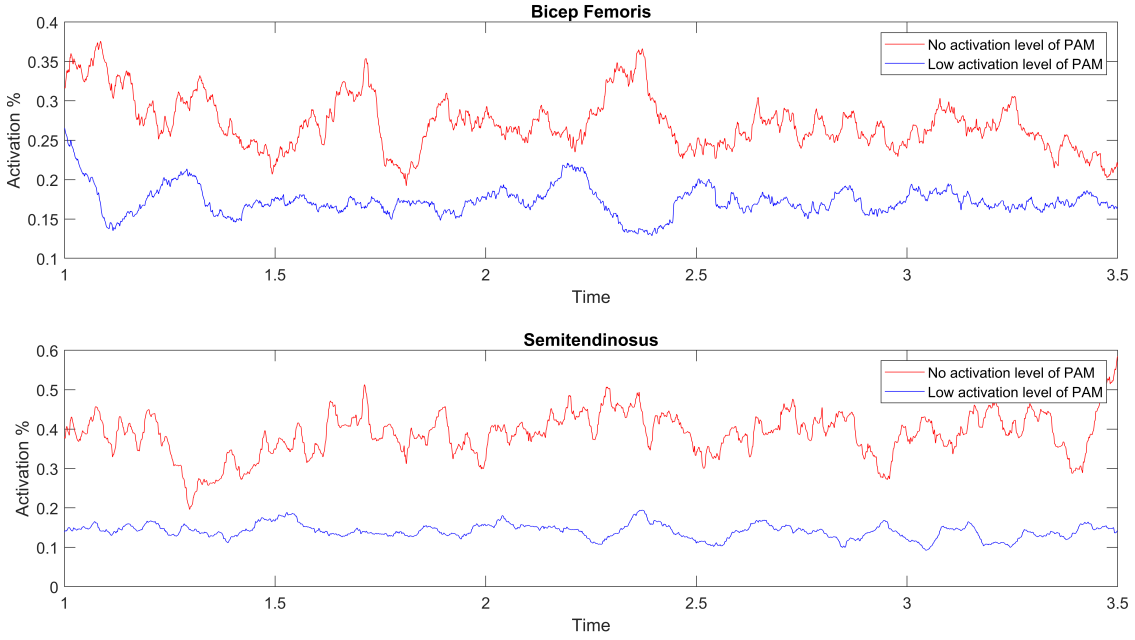

(a)

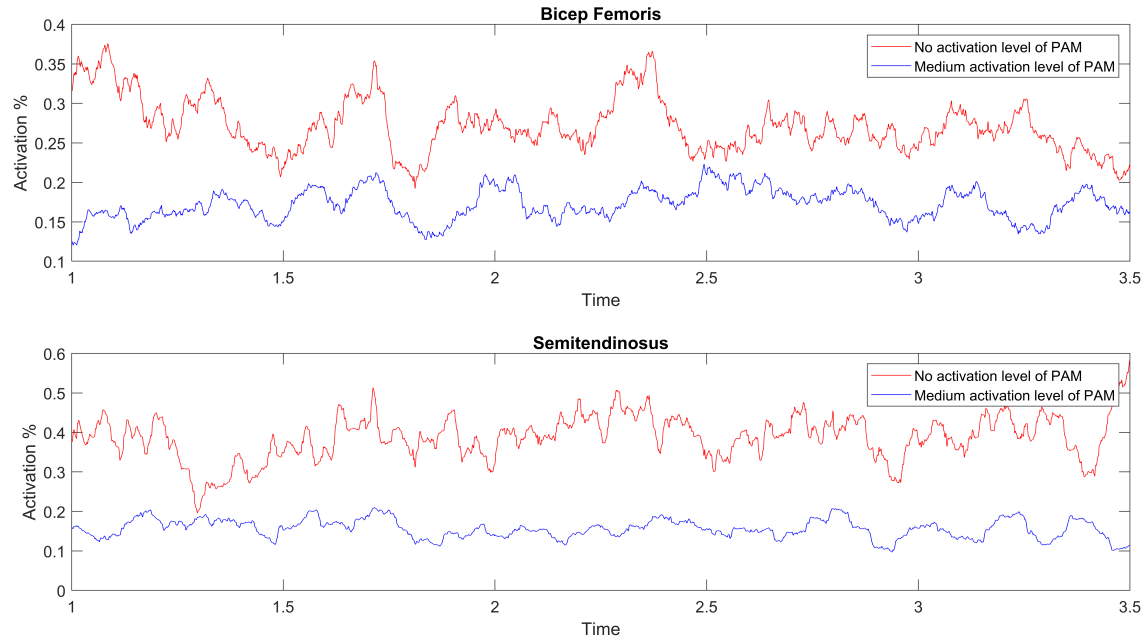

(b)

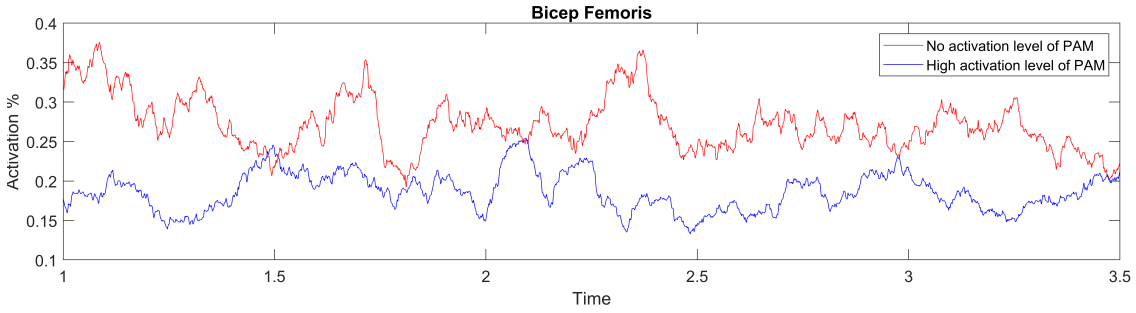

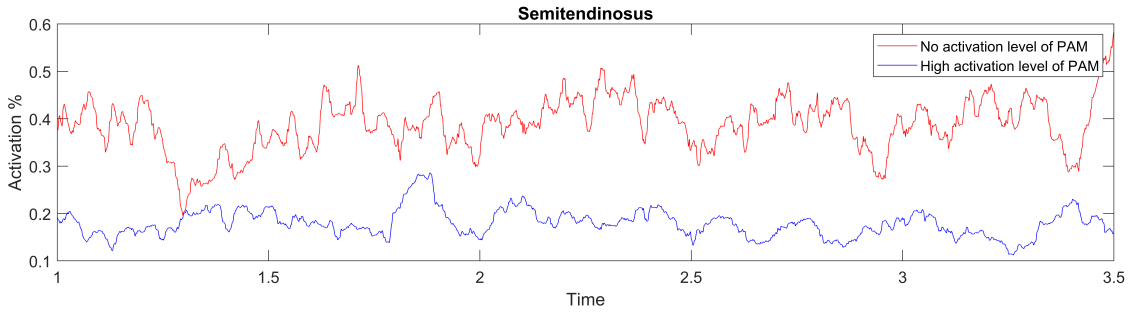

(c)

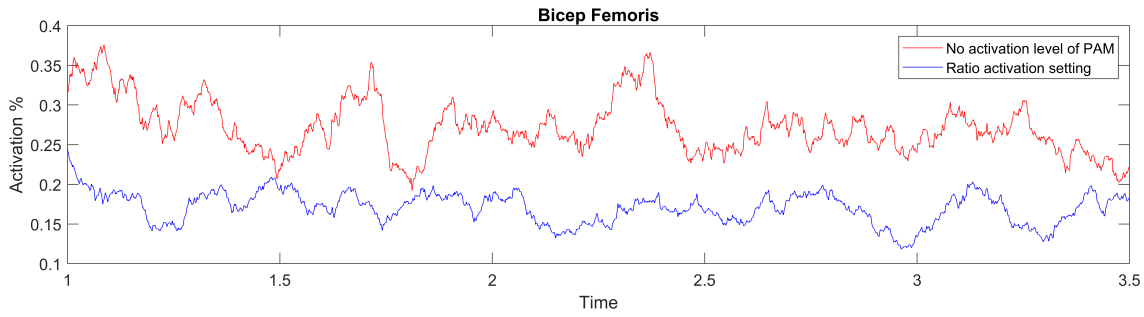

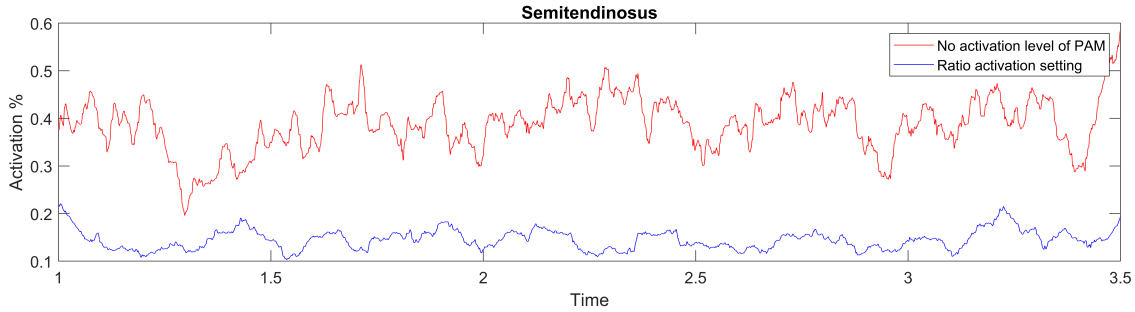

(d)

Figure 7.2: Hamstring activation during seated hamstring curl for different levels of PAM activation for one participant. The activation levels are compared with the signal obtained when the PAMs are unactuated. a) Low activation level (10N). b) Medium activation level (20N). c) High activation level (25N). d) Ratio setting (14.5:3.8N)

Discussion

The Figs. 7.2a, 7.2b and 7.2c show a reduction in hamstring activation when the knee brace is actuated for the different symmetrical actuation levels. Fig. 7.3 shows the mean reduction of the hamstring activation and the mean reduction values are given in Table. 7.1.

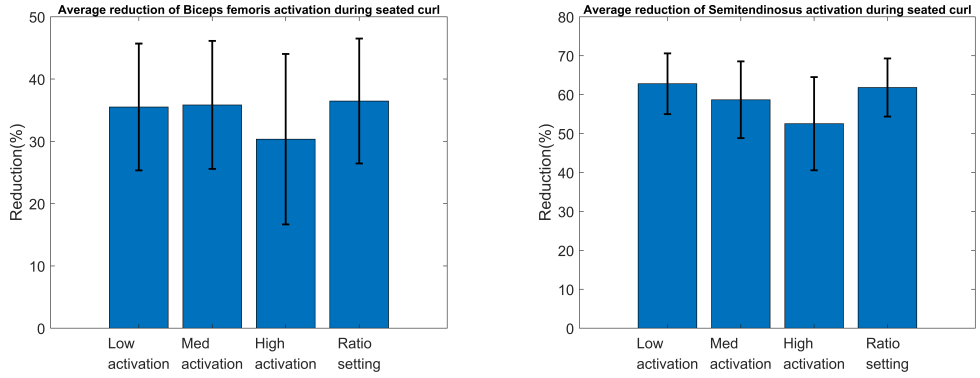

Figure 7.3: Mean reduction of EMG activation level of individual muscles during seated hamstring curl for different activation of PAMs for one participant. a) Biceps Femoris (Lateral hamstring). b) Semitendinosus (Medial hamstring).

It can be seen from the graphs in Fig. 7.2 and Fig. 7.3 that the knee brace is able to reduce the activation of the hamstrings; However, there are certain peaks in the signals. The participants were asked to keep their leg in place during the exercise and when the brace is activated the leg is pulled backwards. As a result to keep the leg in the same place some of the participants tried to stabilize the leg leading to a slight increase in hamstring activation. This can most prominently be seen in the mean reduction for the high activation level of PAMs, where the lower reduction% could be caused due to the stabilization of the leg. The data from the rest of the participants is shown in Appx. B.

Table 7.1: Mean hamstring activation reduction for one participant.

Activation Setting	Reduction in hamstring muscle group	
	Bicep Femoris (Lateral)	Semitendinosus (Medial)
Low Activation	35.5%	62.8%
Medium Activation	35.8%	58.6%
High Activation	30.34%	52.5%
Ratio Setting	36.4%	61.8%

The Table. 7.1 shows the mean reduction for the two hamstring muscles. We observe that the reduction in the Bicep Femoris(BF) is less than the reduction in the Semitendinosus(ST). The BF is located on the lateral side of the knee, while the ST is one of the muscles present in the medial side of the knee. Onishi et al., 2002 in their paper conclude that during the initial angles of flexion the BF is more activated and stretched as compared to the ST muscle. The reverse is true for flexion angles greater than 90°, where the ST have higher activation level as compared to the BF. The static test involving the seated hamstring curl exercise places the knee at a constant angle of approximately 60°. Since the BF muscle is the most activated muscle during the experiment it shows lower reduction as compared to the already less activated ST muscle group.

7.1.3 Gait analysis EMG signals

To be able to compare gait EMG signals a single gait cycle needs to be extracted from each of the acquired signals during the experiment. The EMG system used measures 5 seconds of muscle activation and the time cannot be changed. As a result each acquired signal contains multiple gait cycles. The gait cycles are extracted manually, multiple gait cycles (n=4) for one

participant were averaged and the plot is shown in the Fig. 7.4. The EMG signal for different activation of the PAMs was compared to the EMG signal when the PAM's are not activated. The mean reduction and variance for one participant is shown in Fig. 7.5.

Results

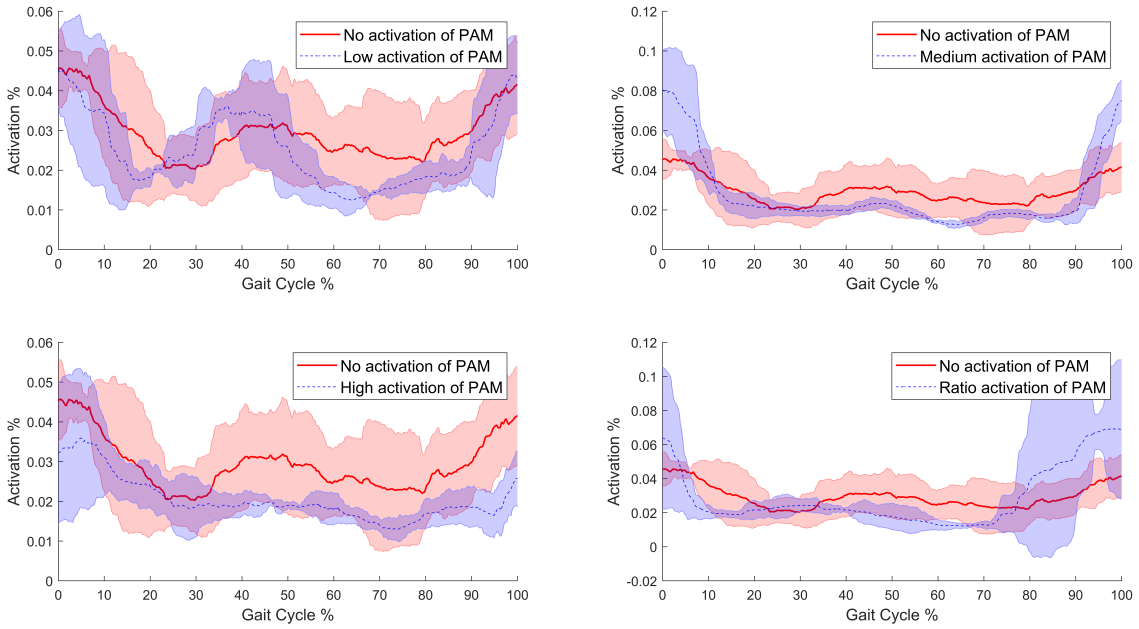

(a)

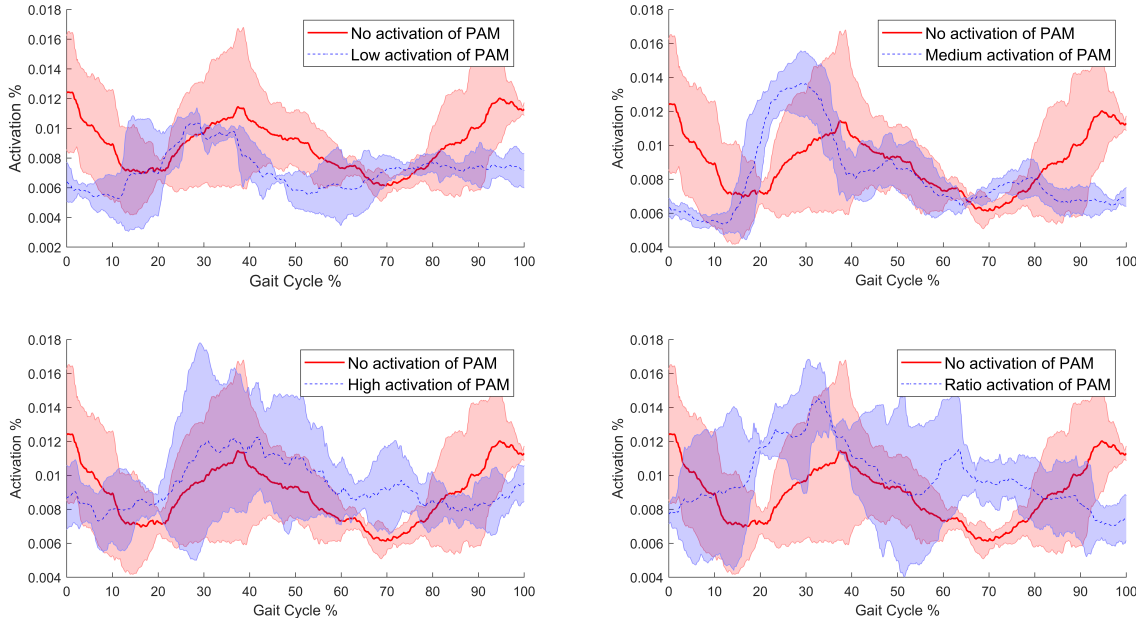

(b)

Figure 7.4: Hamstring activation of individual muscles during gait for different activation of PAMs. a) Biceps Femoris (Lateral hamstring). b) Semitendinosus (Medial hamstring).

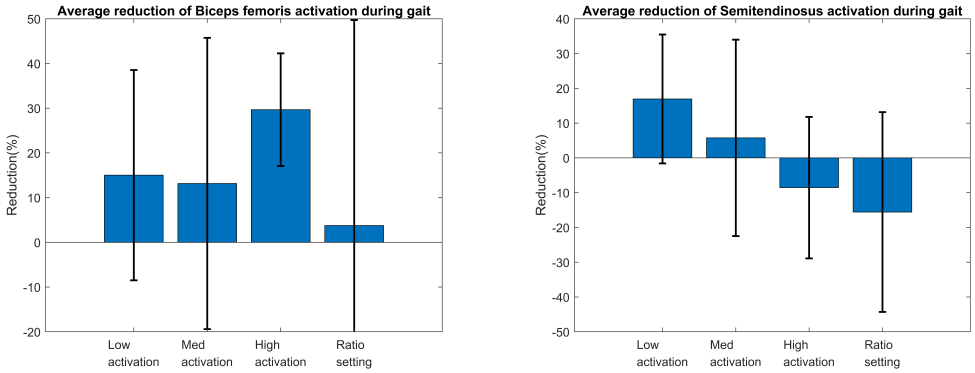

Figure 7.5: Reduction of EMG level of individual muscles during gait for different activation of PAMs. a) Biceps Femoris (Lateral hamstring). b) Semitendinosus (Medial hamstring).

Discussion

The plot for gait analysis shown in Fig. 7.4 were manually extracted to verify the activation pattern of the two hamstring muscles we compare the signal to a template of sEMG signal from the hamstring muscle group during gait which is shown in Fig. 7.6. The template was taken from an article by Sridar et al.,2018, where they develop a soft exosuit for gait assistance. The sEMG plot in the article is attained while wearing a brace like device around the knee. This is why we are able to compare the template with our results as the normal activation patterns of the hamstring are not the same while wearing a brace around the knee.

Data was collected from 4 participants, but only data from 3 participants showed the peaks present during walking from which, the gait cycles could be extracted. One of the participants data showed almost no peaks or distinctive patterns to analyse the gait cycle. This is probably due to the EMG sensors not being placed correctly. It could also be that during walking the adhesive on the sensors may have come loose and hence is not presented. The data of the remaining two participants is given in Appx. B.

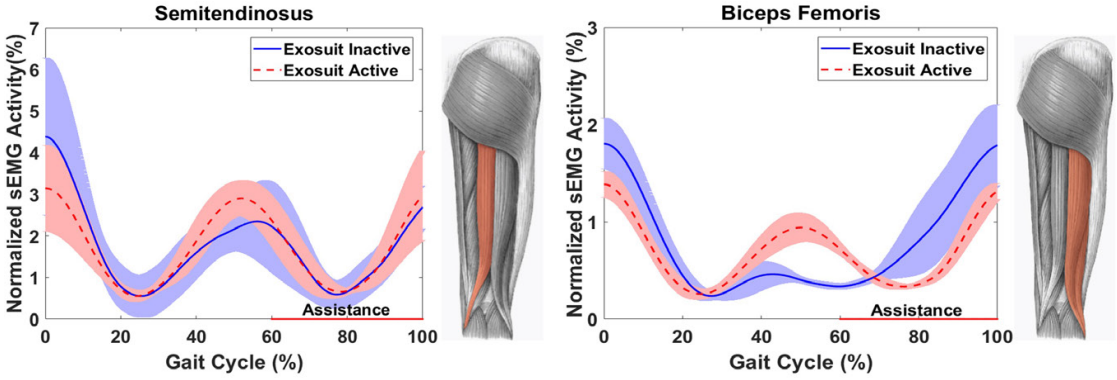

Figure 7.6: Hamstring muscle activation pattern during gait (in blue) for the Biceps Femoris and Semitendinosus muscles. The image has been cropped from Sridar et al., 2018

It can be seen from the plots that activating the brace does lead to reduction of the hamstring activation; However the error margin is quite high as compared to the error seen during the hamstring curl experiment. This we believe is due to the increased stiffness of the brace impeding the normal walking pattern of the participant. Furthermore, when the brace is activated the contraction of the PAMs does not allow the wearer to completely straighten their knee.

This effect can most prominently be seen in Fig. 7.4a where the standard deviation is greater at the beginning and end of the gait cycle when the leg goes into full extension. At greater angles of flexion the PAMs due to their static attachment to the brace, are not able to apply force to the knee joint. This leads us to believe that a dynamic system is required to accommodate the PAMs during flexion/extension of the knee joint.

8 Conclusion and Future scope

In this chapter we present the conclusion and future scope of this thesis. Limitations to the study are also mentioned.

8.1 Conclusion

The rupture of the ACL is of significant importance as the knee joint is one of the most important joints of the body. The knee joint supports most of the total body weight everyday in daily activities. A ligament tear in such a joint can lead to long term consequences such as knee arthritis. The ACLs structure and position make it the most injury prone of the few ligaments present in the knee. Reconstruction of the ACL, though a viable option, is mostly recommended to patients with high activity levels such as athletes. We aimed at developing a soft robotic knee brace to reduce the effect of the ACL rupture.

To this extent the first research question was to see the changes caused due to the ACL rupture to the kinematics or biomechanics of the knee. We found that the ACL not only prevents the anterior motion of the tibia but also activates the hamstring muscle group to help reduce this motion. A severed ACL results in late activation of the hamstrings which decreases the overall stability of the joint. It is seen that patients with a severed ACL may choose an incorrect muscle coordination method due to pain or an uncomfortable feeling in their joint, leading to further wear and tear of the articular tibiofemoral cartilage. During rehabilitation ACLD patients are made to strengthen their hamstring muscles for increasing the stability of the joint and also to incorporate the correct muscle coordination. The rehabilitation process is lengthy and takes time before the patients can develop their hamstrings and activate them earlier. As such we believe that by assisting the hamstring muscle group we can reduce the effect of the ligament rupture.

Knee braces are available which say that they reduce the strain in the knee joint caused by the ruptured ACL; However, the effect of the braces on the surrounding articulates is not known.

The second research question was to develop a knee brace which is compatible in an MRI machine to see the effect of the brace on the surrounding underlying articulates. To develop a functional brace to be MR compatible the actuators need to be MR compatible as well and must be able to exert considerable amount of force, considering the amount of forces produced by our muscles. This lead us to fabricate our own PAMs which are able to generate forces of upto 50N at 2 Bars of pneumatic pressure. These PAMs were integrated onto an available brace using support structures which were either 3D printed or laser cut from plastic. We attach the PAMs for specific angles of flexion of the knee joint. This is due to the active contraction of the PAMs, which require a dynamic system to shift the attachment sites for different angles of flexion.

The third research question was to see the effect of our brace in reducing the instability in an ACL ruptured knee. To prove the efficacy of our brace we present two kinds of experiments which we believe will show the competence of our brace in reducing the instability caused by an ACL rupture and also, be able to see the effect on surrounding articulates. The first experiment consisted of a sEMG static test during a seated curl exercise and an active test, performed during walking. The test was done on participants with healthy knees to see the effect of our brace on hamstring activation. We see from the EMG results of the static experiment that the brace does reduce the activation of the hamstring muscles group, this shows that the brace can assist the hamstring muscle group and can provide the required forces to do so. The EMG signals during walking show that the brace is more effective at reducing the hamstring activation at lower PAM forces but, at higher forces it impedes the gait cycle as the wearer can no longer extend their knee completely. Suggesting that a dynamic system is required which could alter the stiffness

of the PAMs based on the flexion angle. The second experiment that we propose is to evaluate the brace based on a Lachman test, where the motion of the tibia is assessed. The Lachman test consisted of applying an anterior force on the tibia, knees with a severed ACL show an increase in bone motion as compared to healthy knees. The porto knee testing device explained in Ch. 6 can be used to see if the brace is able to reduce the laxity of the ACLD knee when compared to a healthy knee. Being MR compatible we would also be able to see if the brace is placing unwanted stresses on the underlying articular tibiofemoral cartilage.

8.1.1 Limitations of study

There are a few limitations to our study during the development of the soft robotic knee brace.

Experimentation on ACL ruptured patients would give a more conclusive effect of our brace on hamstring activation when the ACL is ruptured. Involving ACLD patients required METC approval and due to time restrictions, healthy participants were used instead.

The EMG system used only consisted of two channels making it possible to measure only two hamstring muscles out of all the various the muscle groups surrounding the knee. Measurement of the various muscle groups would further provide a better understanding of the activation pattern of all the muscles supporting the knee joint.

The gait cycles for the gait analysis experiment were manually extracted from the EMG data based on a repeating trend in the EMG pattern. Most gait analysis studies use either a force plate to mark the beginning and end of a gait cycle or are able to extract the gait cycles based on measured angle of knee flexion. As a result the gait cycles may not be properly synced and since the EMG signal is effected by the brace, we cannot compare the pattern to regular templates of gait cycles presented in literature.

8.2 Future Scope

Based on the final application of the knee brace and considering the results from the EMG experiment there are several future recommendations to be made. Due to limited availability of an MRI system, we were not able to evaluate the motion of the bones in an MRI using the porto knee testing device. This would certainly give a better idea on how the brace affects the underlying passive structures and can be used to modify the design further.

The second recommendation for future work would be to design a dynamic system for the entire range of flexion. Currently, the brace is only activated for certain angles of flexion. A dynamic actuation control of the PAMs can be used to change the stiffness of the brace as a whole allowing for better use during daily activities such as walking and climbing up stairs.

Implementing dynamic control into the system would require a form of feedback. Measurement of the knee flexion angle would provide a conclusive feedback method to control the brace. Implementation of a system to measure the knee flexion angle has already been implemented by Andrea Ryolo. He used a potentiometer based system with the geared hinges to measure the angle of the knee. The system developed by him is not MR compatible and can currently only be used as a tool for feedback in the case of a dynamic system.

A motion profile of the bones for an ACL rupture patient should be estimated during daily activities. This would allow for a better understanding on the required forces for the full range of flexion.

Hysteresis during characterization of the PAMs was neglected. This was because our experiments consisted of discrete activation levels in time; However, while implementing dynamic control to the brace, hysteresis should be taken into consideration.

Another recommendation would be to use a more detailed EMG system to check the activation of the surrounding muscle groups as well and not just the hamstring muscle group. The

muscles around the knee work together to provide the required kinematics required to complete a task. A detailed study on the activation patterns of different muscle groups would provide a better understanding on the working of the brace.

Lastly, the design of the brace as a whole can be modified. The PAMs used in the brace are actuated through an external pressure supply limiting the wear-ability of the brace. The amount of pressure required by the brace is less and a portable pneumatic compressor can be integrated into the brace. The PAMs themselves increase the lateral size of the brace, the design could be made smaller allowing for better user comfort.

A Experiment protocols

A.1 sEMG Protocol

A.1.1 Seated hamstring curl with resistance band

1. The participant is to perform a hamstring curl using a resistance band attached to a rigid support. Ask the participant to sit down for this study.
2. Dip the electrodes and arm strap in salt water.This is done to improve the conductivity of the electrodes.
3. The active electrodes are then placed over the main belly of the Semitendinosus (ST) and the Bicep femoris long head (BFlh) as seen in fig A.1. While placing the electrodes make sure to clean the area around the electrodes.
4. Connect the earth electrode to the amplifier and the other end to the arm strap.
5. Place the arm strap around the wrist of the participant.
6. The brace is to be worn. After its worn attach the support structures with the artificial muscles attcahed at the configuration for 60°.

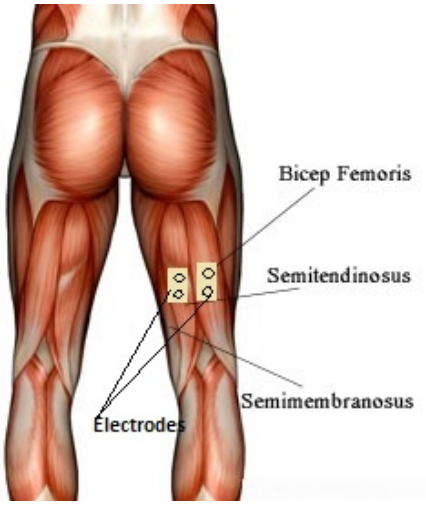

Figure A.1: Placement of electrodes.

7. Connect the electrodes to the EMG amplifier. Two white electrodes for sensing and one earth electrode.
8. Connect the amplifier to the laptop containing the systemPLUS Evolution software and licence through the USB converter.
9. Start the systemPLUS Evolution software and enter the participants details.
10. Set the targeted muscle group in the software.
11. Press spacebar to start recording when ready.
12. The first recording will be when the participants muscles are completely relaxed with no voluntary muscle activation. This provides us with the baseline reference for the noise in the system.

13. The participant is then asked to place bend the knee to an angle of 60° and the hip angle at 110°. This is done to ensure the maximum activation of the hamstrings in the whole range of motion.

14. The participant is then asked to contract his hamstring muscles as much as possible without movement of the leg. This is done to obtain the maximum voluntary isometric contraction level of the muscle, which provides us with the maximum activation level of the muscle and is then used for normalization of later signals.

15. The resistance band is pulled to be able to generate a force of 50N and the location is marked on the floor. The participant is to put his leg with the brace through the resistance band and keep his foot over a marked location with knee and hips at 60° and 110° respectively.

16. Four conditions are recorded 3 times each with a rest of 2 minutes between each condition. The conditions are:

    - No activation of the artificial muscles.
    - Low activation of the artificial muscles at a force of 10N.
    - Medium activation of the artificial muscles at a force of 20N.
    - High activation of the artificial muscles at a force of 25N.
    - Ratio setting with medial PAM at 14N and lateral PAM at 4N respectively

17. Save all the data and export each of them as an ASCII file.

A.1.2 Gait analysis

1. The participant is to walk on a treadmill while wearing the brace.

2. Prior to wearing the brace the participant is asked to walk on the treadmill to find the speed they are most comfortable with. The speed is set so that the participant can walk at a normal pace while not moving with respect to the treadmill.

3. The EMG sensors are placed in the same location as in the seated hamstring curl.

4. The participant is first asked to stand straight and loosen the hamstring muscles while standing straight. This provides us with a baseline for our experiment.

5. The participant is then asked to walk on the treadmill at a slow pace then normal. This is performed to obtain the normalization factor.

6. The speed is then increased to the normal value. The participant is to keep walking until all readings are taken.

7. Readings are taken for different levels of activation of the artificial muscles at zero, low, medium and high activation.

8. Three different readings are taken for each level of activation.

9. Save all the data and export each of them as an ASCII file.

B EMG signals

In this section of the appendix we present the EMG signals for both exercises for the remaining participants.

B.1 Seated hamstring curl

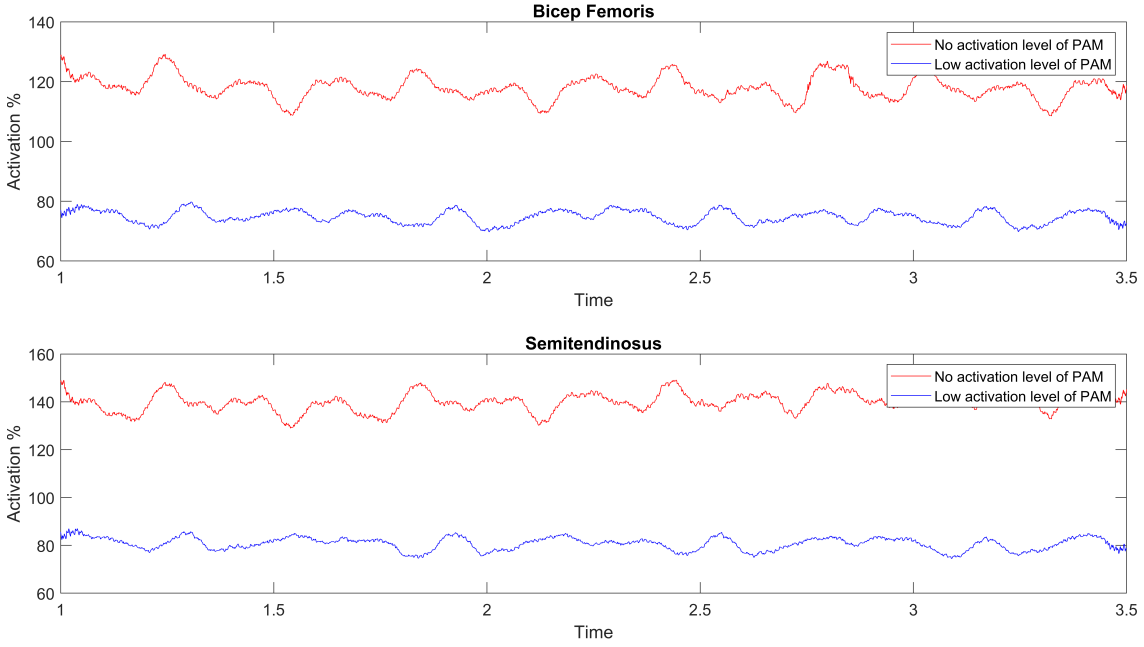

(a)

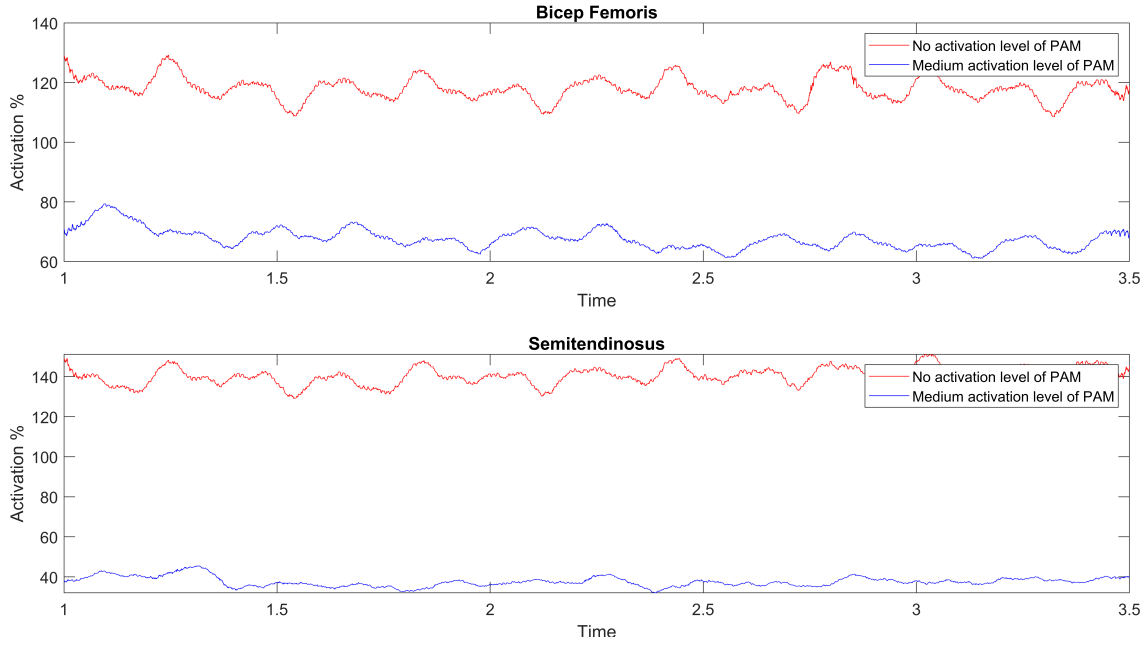

(b)

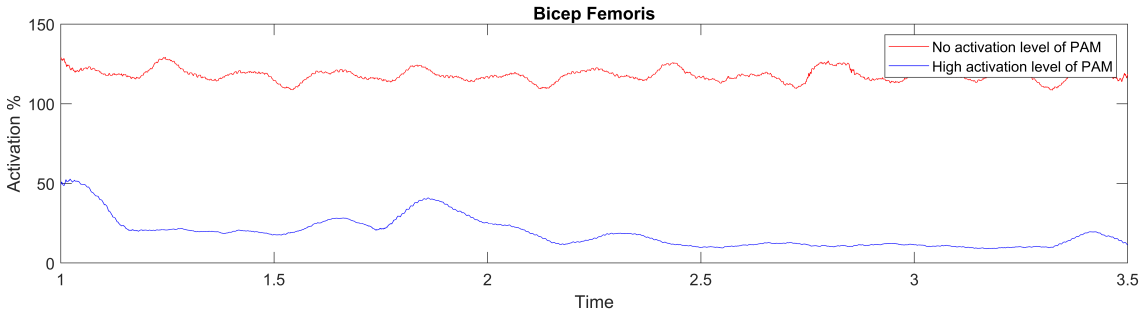

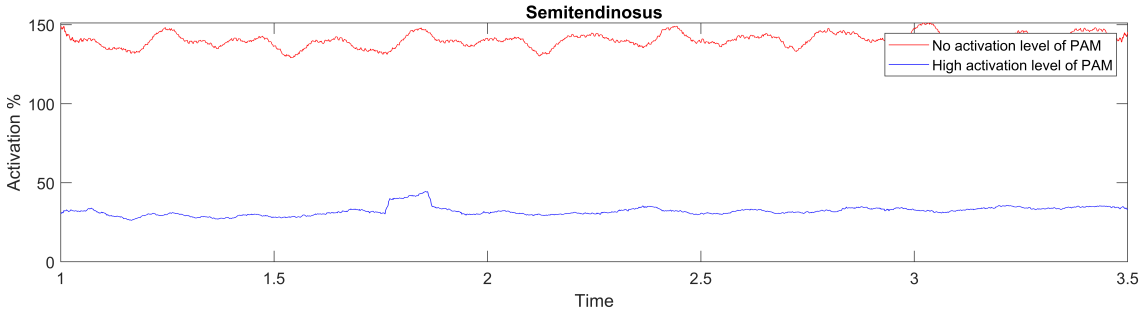

(a)

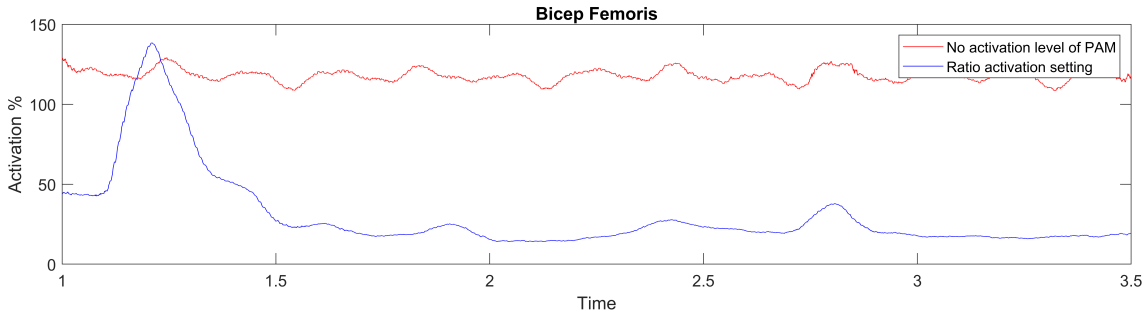

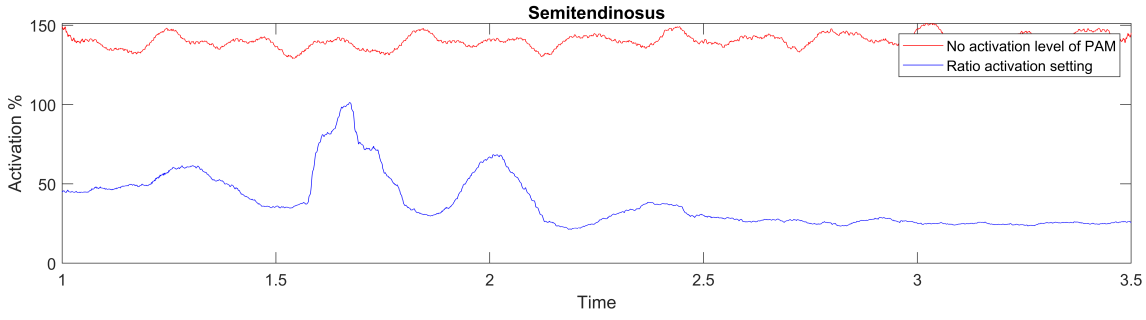

(b)

Figure B.2: Hamstring activation during seated hamstring curl for different levels of PAM activation for participant 2. The activation levels are compared with the signal obtained when the PAMs are unactuated. a) Low activation level (10N). b) Medium activation level (20N). c) High activation level (25N). d) Ratio setting (14.5:3.8N)

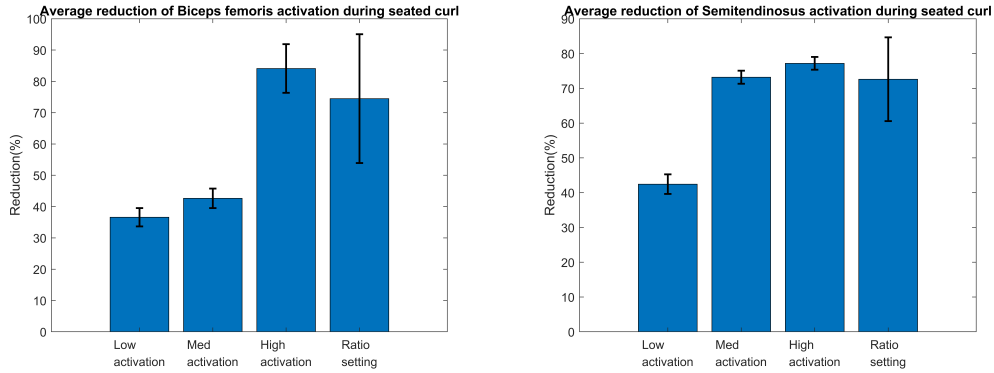

(a) **(b)**

Figure B.3: Mean reduction of EMG activation level of individual muscles during seated hamstring curl for different activation of PAMs for participant2. a) Biceps Femoris (Lateral hamstring). b) Semitendinosus (Medial hamstring).

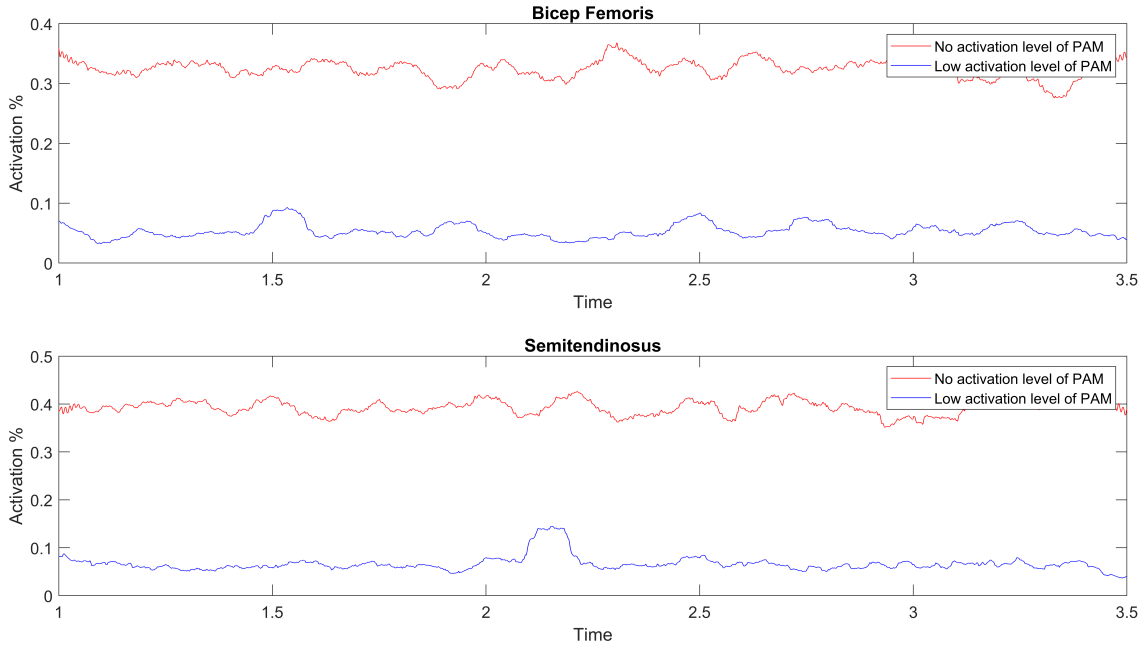
Bicep Femoris
No activation level of PAM
Low activation level of PAM
Activation %
Time
Semitendinosus
No activation level of PAM
Low activation level of PAM
Activation %
Time

(a)

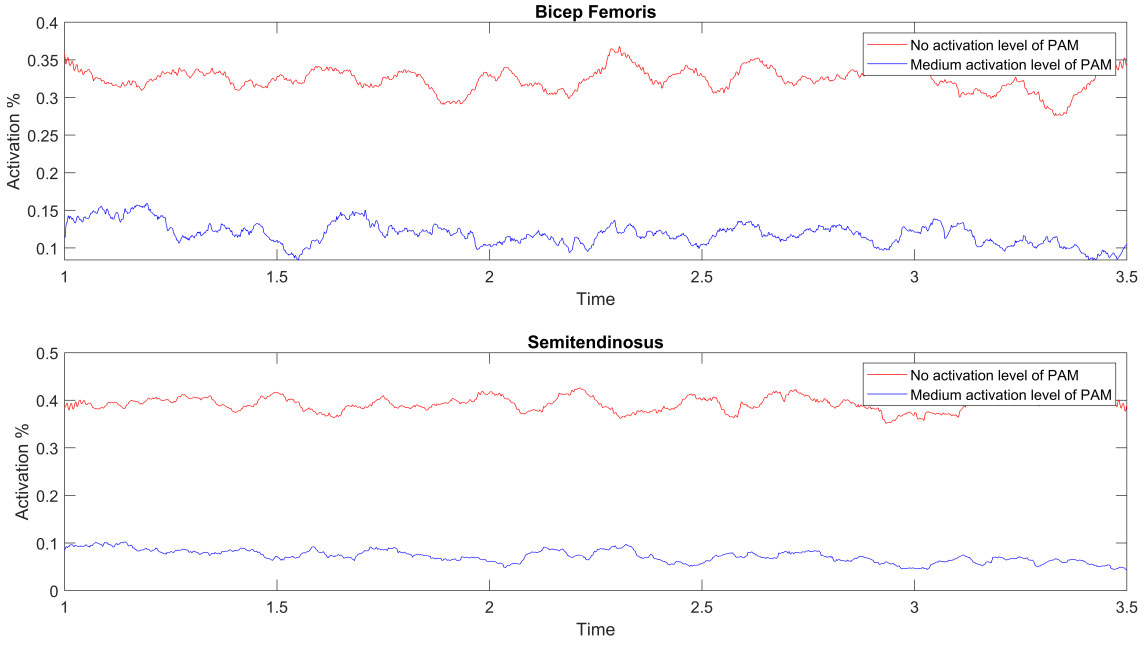
Bicep Femoris
No activation level of PAM
Medium activation level of PAM
Activation %
Time
Semitendinosus
No activation level of PAM
Medium activation level of PAM
Activation %
Time

(b)

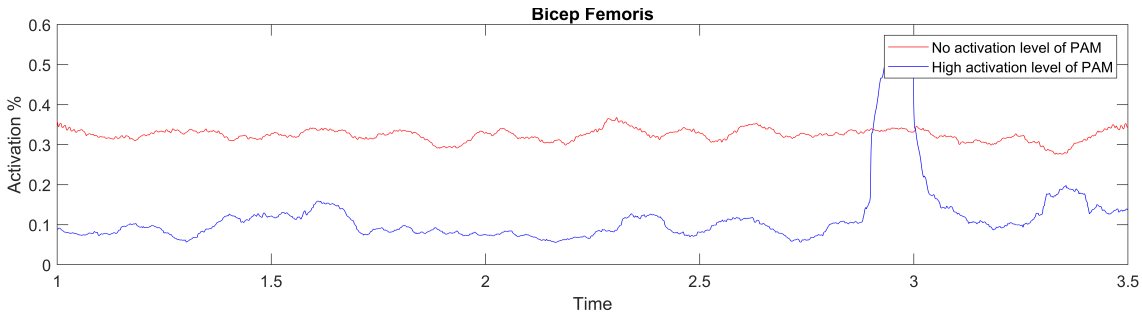

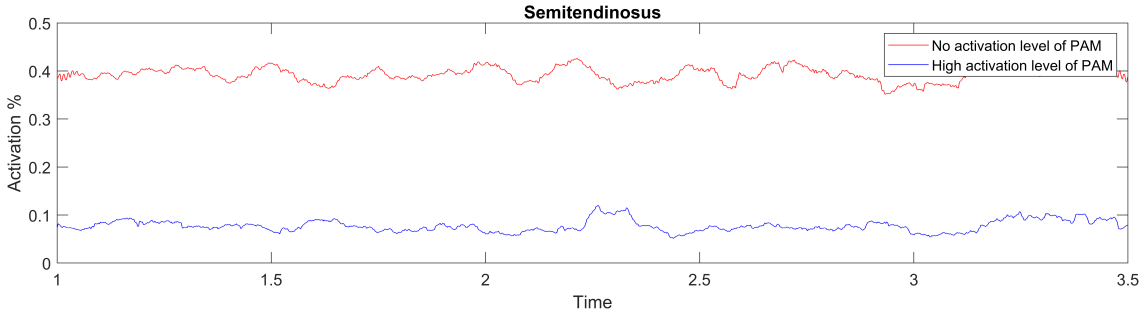

(a)

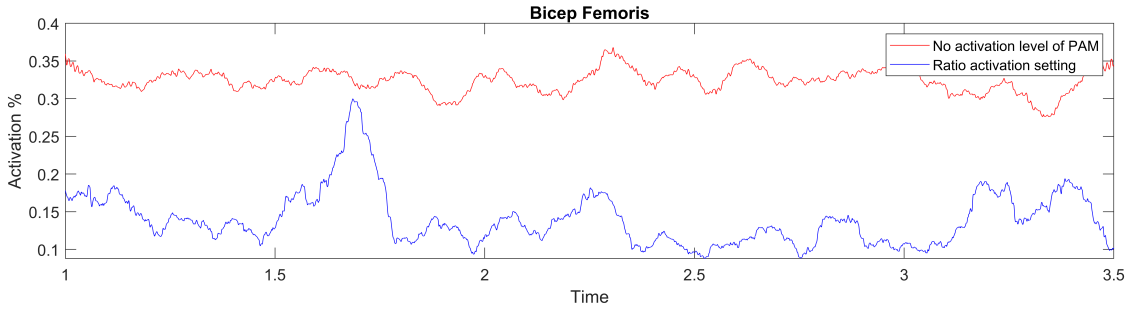

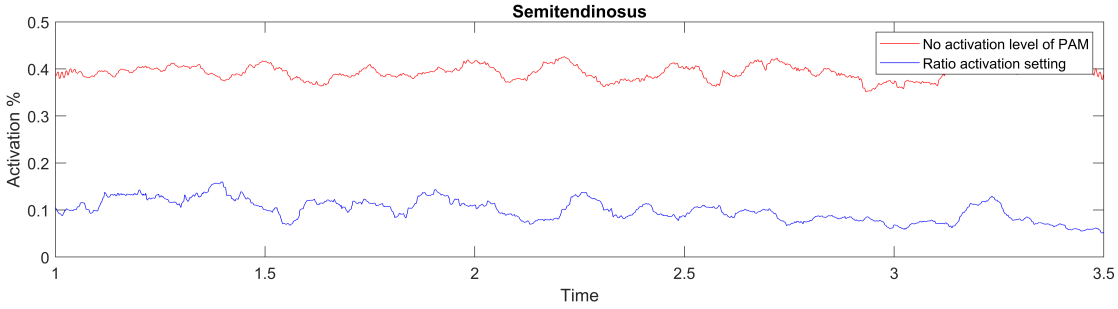

(b)

Figure B.5: Hamstring activation during seated hamstring curl for different levels of PAM activation for participant 3. The activation levels are compared with the signal obtained when the PAMs are unactuated. a) Low activation level (10N). b) Medium activation level (20N). c) High activation level (25N). d) Ratio setting (14.5:3.8N)

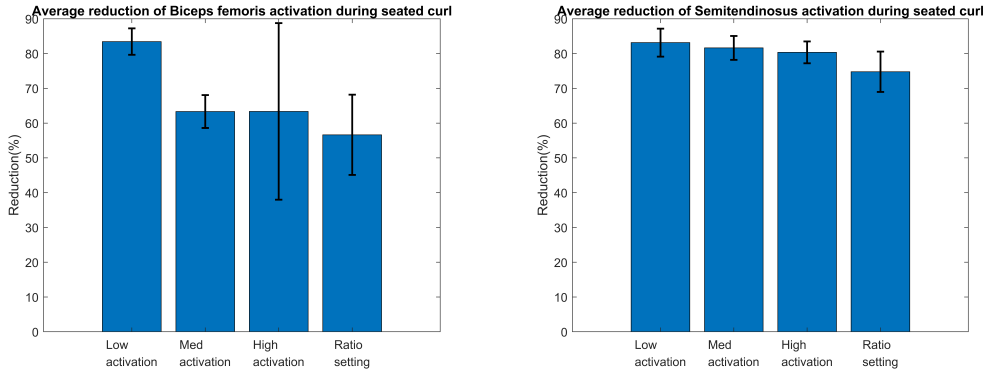

(a) **(b)**

Figure B.6: Mean reduction of EMG activation level of individual muscles during seated hamstring curl for different activation of PAMs for participant 3. a) Biceps Femoris (Lateral hamstring). b) Semitendinosus (Medial hamstring).

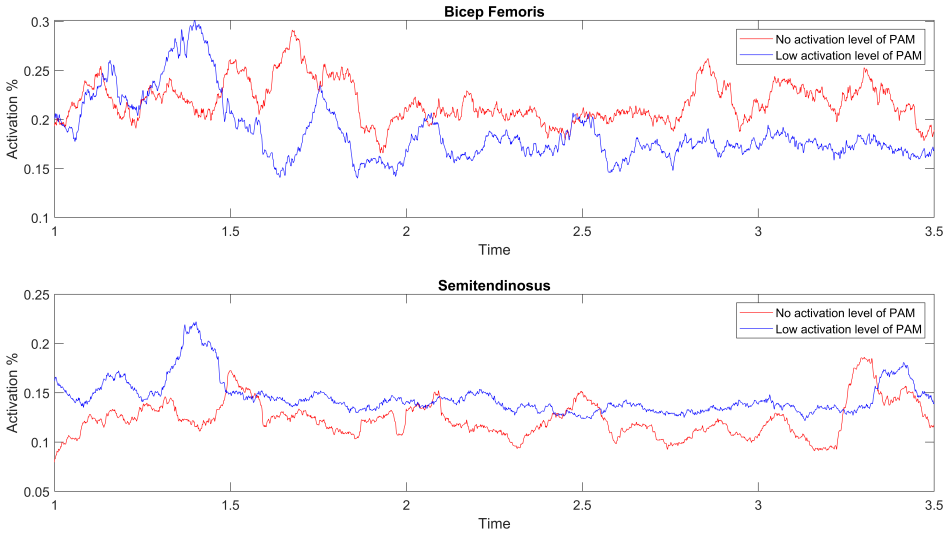
Bicep Femoris
No activation level of PAM
Low activation level of PAM
Activation %
Time
Semitendinosus
No activation level of PAM
Low activation level of PAM
Activation %
Time

(a)

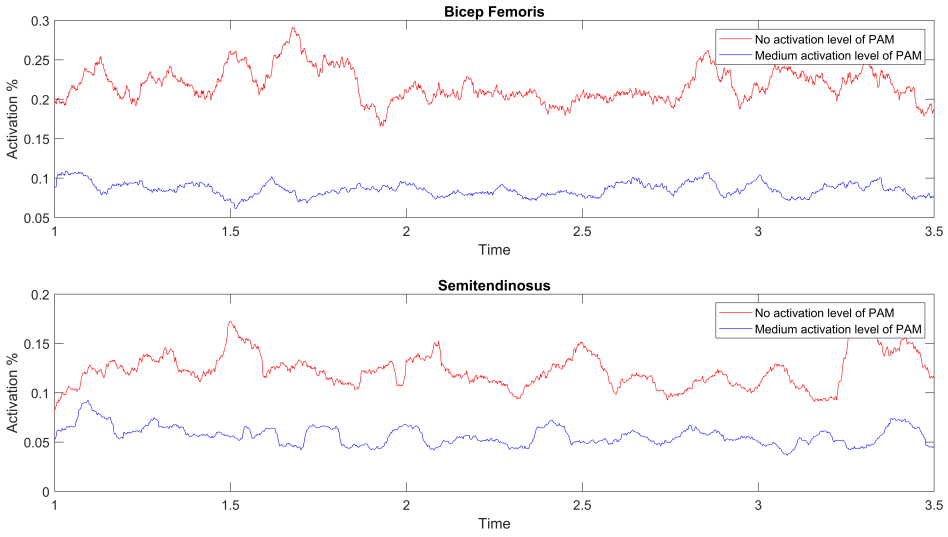
Bicep Femoris
No activation level of PAM
Medium activation level of PAM
Activation %
Time
Semitendinosus
No activation level of PAM
Medium activation level of PAM
Activation %
Time

(b)

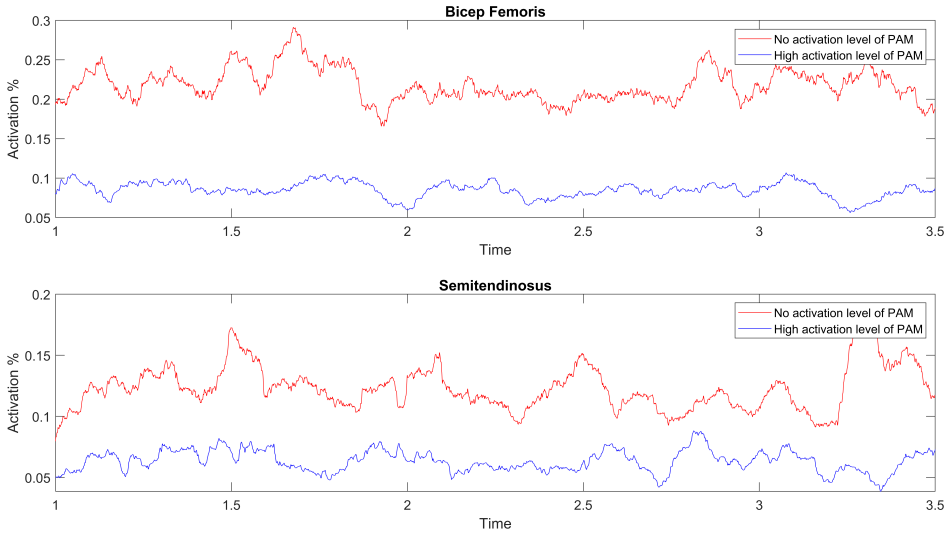

(a)

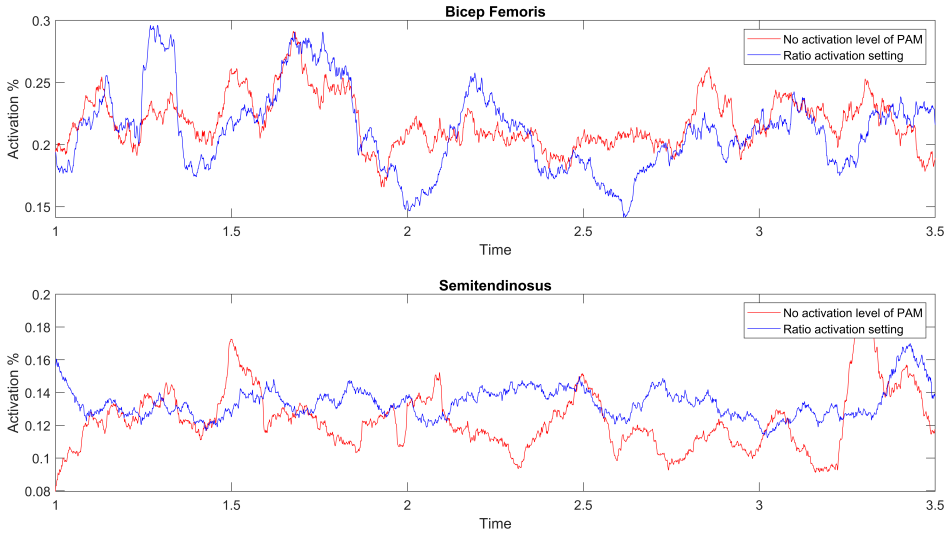

(b)

Figure B.8: Hamstring activation during seated hamstring curl for different levels of PAM activation for participant 4. The activation levels are compared with the signal obtained when the PAMs are unactuated. a) Low activation level (10N). b) Medium activation level (20N). c) High activation level (25N). d) Ratio setting (14.5:3.8N)

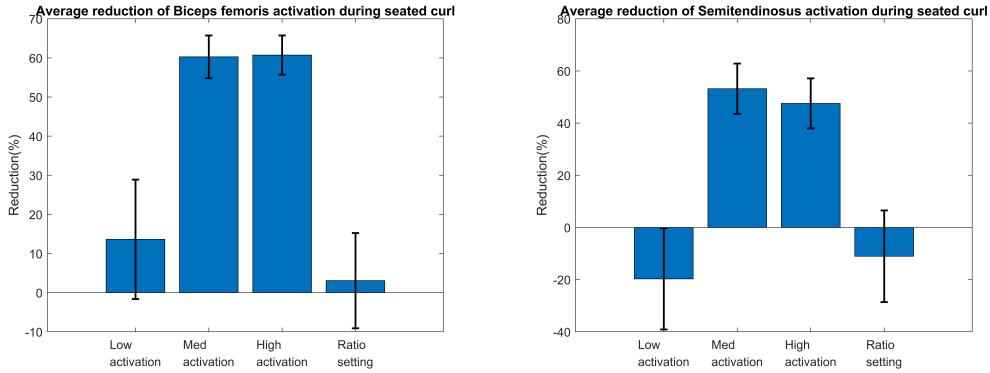

Figure B.9: Mean reduction of EMG activation level of individual muscles during seated hamstring curl for different activation of PAMs for participant 4. a) Biceps Femoris (Lateral hamstring). b) Semitendinosus (Medial hamstring).

B.2 Gait analysis

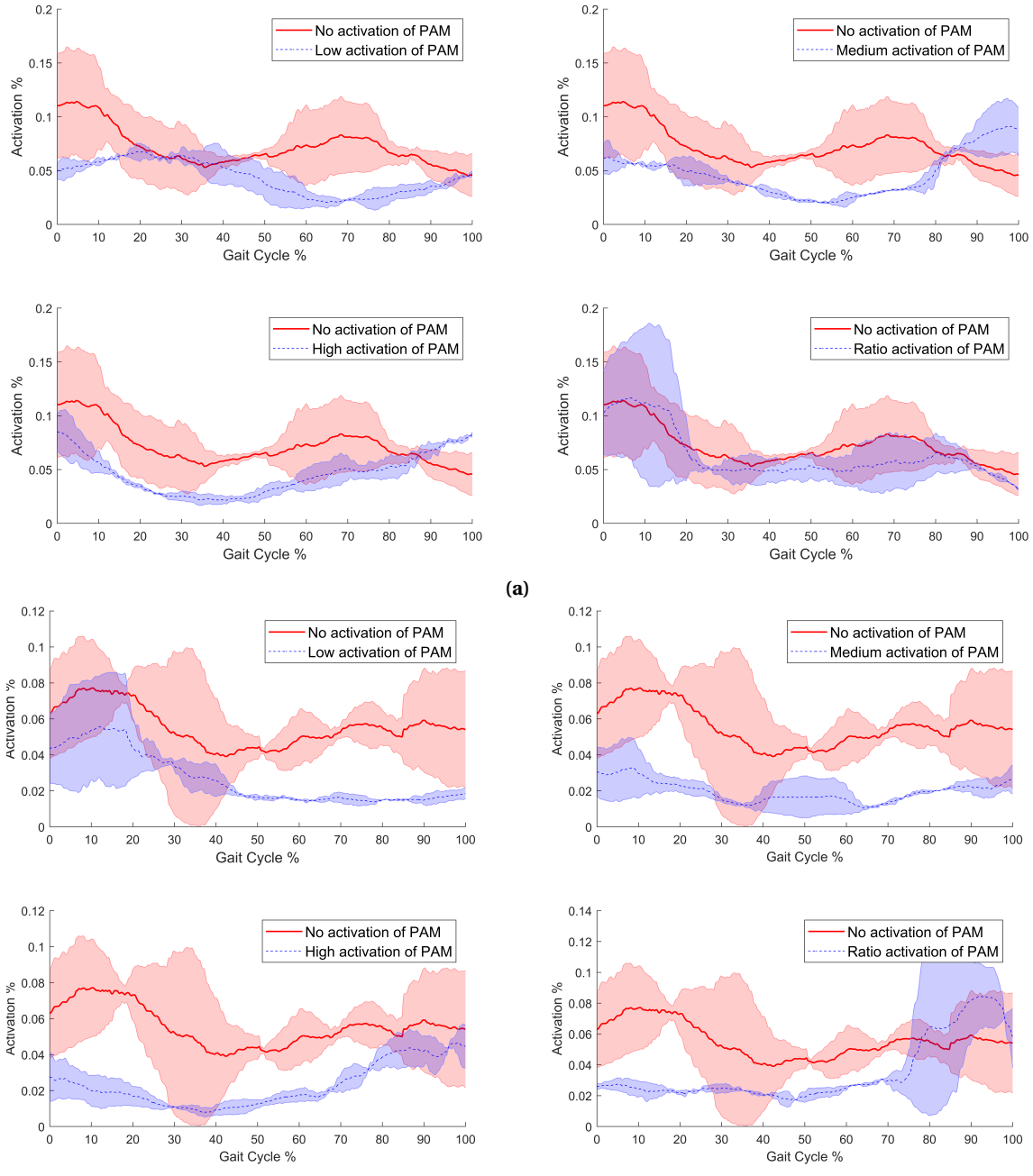

Figure B.10: Hamstring activation of individual muscles during gait for different activation of PAMs for participant 2. a) Biceps Femoris (Lateral hamstring). b) Semitendinosus (Medial hamstring).

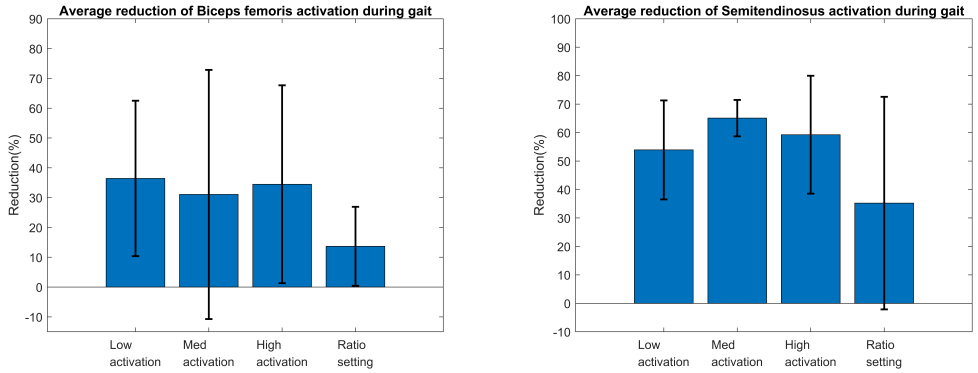

Figure B.11: Reduction of EMG level of individual muscles during gait for different activation of PAMs for participant 2. a) Biceps Femoris (Lateral hamstring). b) Semitendinosus (Medial hamstring).

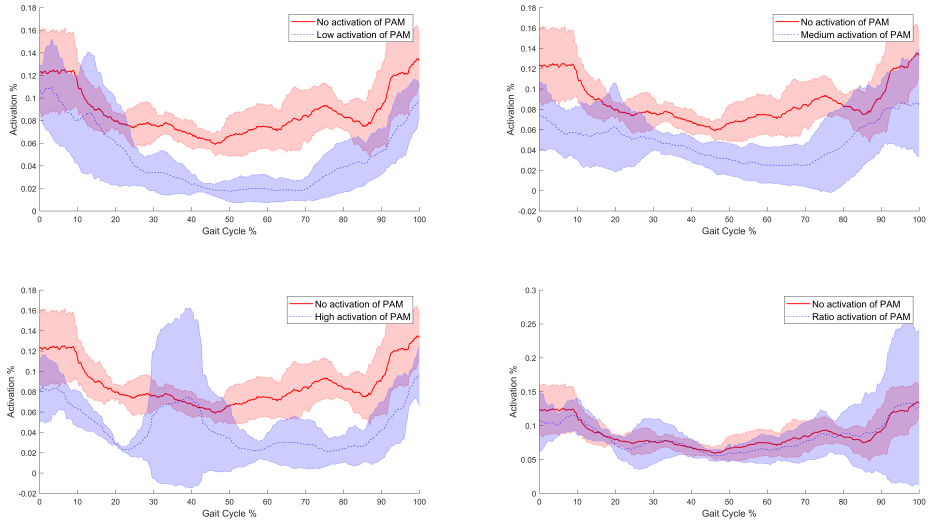

(a)

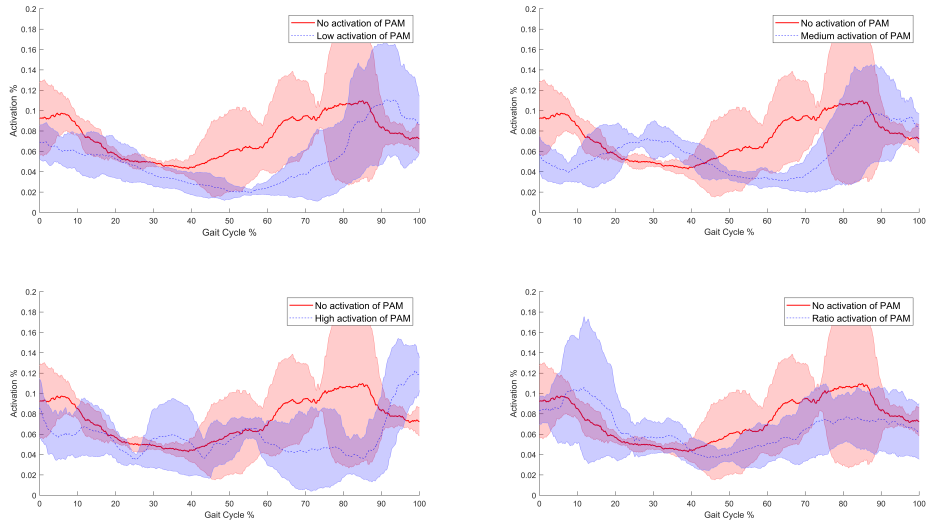

(b)

Figure B.12: Hamstring activation of individual muscles during gait for different activation of PAMs for participant 3. a) Biceps Femoris (Lateral hamstring). b) Semitendinosus (Medial hamstring).

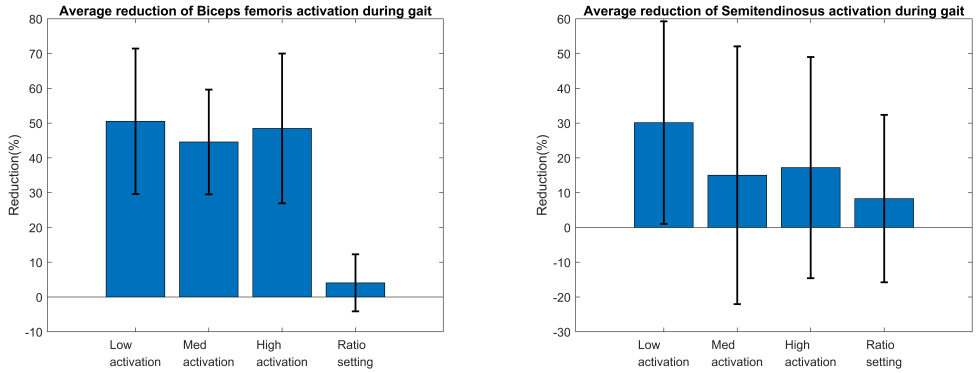

Figure B.13: Reduction of EMG level of individual muscles during gait for different activation of PAMs for participant 3. a) Biceps Femoris (Lateral hamstring). b) Semitendinosus (Medial hamstring).

Bibliography

Aagaard, P., E. Simonsen, J. Andersen, S. Magnusson, F. Bojsen-Møller and P. Dyhre-Poulsen (2000), Antagonist muscle coactivation during isokinetic knee extension, **vol. 10**, no.2, pp. 58–67.

Advisor, C. (2019), Tests to assess ACL rupture, [Online; accessed 17-Sept-2019]. https://www.clinicaladvisor.com/slideshow/slides/tests-to-assess-acl-rupture/

Andrikopoulos, G., G. Nikolakopoulos and S. Manesis (2011), A survey on applications of pneumatic artificial muscles, in 2011 19th Mediterranean Conference on Control & Automation (MED), IEEE, pp. 1439–1446.

Arneja, S. and J. Leith (2009), Validity of the KT-1000 knee ligament arthrometer, **vol. 17**, no.1, pp. 77–79.

Aweid, O., H. Osmani and J. Melton (2019), Biomechanics of the knee, **vol. 33**, no.4, pp. 224 – 230, ISSN 1877-1327, doi:https://doi.org/10.1016/j.mporth.2019.05.004. http://www.sciencedirect.com/science/article/pii/S1877132719300387

BraceAbility (2004), Range of Motion Knee Stabilizer for Athletes & Contact Sports, united States of America.

Brandsson, S., J. Karlsson, L. Swärd, J. Kartus, B. I. Eriksson and J. Kärrholm (2002), Kinematics and laxity of the knee joint after anterior cruciate ligament reconstruction: pre-and postoperative radiostereometric studies, **vol. 30**, no.3, pp. 361–367.

Bryant, A. L., M. W. Creaby, R. U. Newton and J. R. Steele (2008), Dynamic restraint capacity of the hamstring muscles has important functional implications after anterior cruciate ligament injury and anterior cruciate ligament reconstruction, **vol. 89**, no.12, pp. 2324–2331.

Carboflex (2019), Carboflex Advance Functional Knee Brace, united Kingdom.

Carlo Ferraresi, W. F., W. Walter Franco and A. Bertetto (2001), Flexible pneumatic actuators: a comparison between the McKibben and the straight fibres muscles, **vol. 13**, no.1, pp. 56–63.

Cerulli, G., G. Placella, E. Sebastiani, M. M. Tei, A. Speziali and F. Manfreda (2013), ACL reconstruction: choosing the graft, **vol. 1**, no.1, p. 18.

Ching-Ping Chou and B. Hannaford (1996), Measurement and modeling of McKibben pneumatic artificial muscles, **vol. 12**, no.1, pp. 90–102, ISSN 1042-296X, doi:10.1109/70.481753.

Commons, W. (2019), File:Põlveliiges.png — Wikimedia Commons, the free media repository, [Online; accessed 2-July-2019]. https://commons.wikimedia.org/w/index.php?title=File:P%C3%B5lveliiges.png&oldid=344999014

Daerden, F. and D. Lefeber (2002), Pneumatic artificial muscles: actuators for robotics and automation, **vol. 47**, no.1, pp. 11–21.

Dargel, J., M. Gotter, K. Mader, D. Pennig, J. Koebke and R. Schmidt-Wiethoff (2007), Biomechanics of the anterior cruciate ligament and implications for surgical reconstruction, **vol. 2**, no.1, pp. 1–12, ISSN 1828-8928, doi:10.1007/s11751-007-0016-6. https://doi.org/10.1007/s11751-007-0016-6

De Luca, C. J., L. D. Gilmore, M. Kuznetsov and S. H. Roy (2010), Filtering the surface EMG signal: Movement artifact and baseline noise contamination, **vol. 43**, no.8, pp. 1573–1579.

De Luca, C. J., M. Kuznetsov, L. D. Gilmore and S. H. Roy (2012), Inter-electrode spacing of surface EMG sensors: reduction of crosstalk contamination during voluntary contractions,

vol. 45, no.3, pp. 555–561.

Donjoy (2019), Donjoy Full Force Short Knee Brace - Ligament & Cartilage Knee Support - Injury Rehab & Recovery. Product Code: 11-X.

Doumit, M., A. Fahim and M. Munro (2009), Analytical modeling and experimental validation of the braided pneumatic muscle, **vol. 25**, no.6, pp. 1282–1291.

Espregueira-Mendes, J. (2012), A new tool to objective assessment of rotational instability and ACL/PCL deficient knees inside magnetic resonance imaging or CT scan, [Online; accessed 03-Sept-2019].
http://www.portotestingdevice.com/?p=2&n=pktd

Espregueira-Mendes, J., H. Pereira, N. Sevivas, C. Passos, J. C. Vasconcelos, A. Monteiro, J. M. Oliveira and R. L. Reis (2012), Assessment of rotatory laxity in anterior cruciate ligament-deficient knees using magnetic resonance imaging with Porto-knee testing device, **vol. 20**, no.4, pp. 671–678, ISSN 1433-7347, doi:10.1007/s00167-012-1914-9.
https://doi.org/10.1007/s00167-012-1914-9

Fairview (2019), Hamstring Curl (Strength), [Online; accessed 15-Sept-2019].
https://www.fairview.org/patient-education/90814

Flandry, F. and G. Hommel (2011), Normal anatomy and biomechanics of the knee, **vol. 19**, no.2, pp. 82–92.

Gaylord, R. H. (1958), Fluid actuated motor system and stroking device, uS Patent 2,844,126.

Haisman, M. (1988), Determinants of load carrying ability, **vol. 19**, no.2, pp. 111–121.

Halaki, M. and K. Ginn (2012), Normalization of EMG Signals: To Normalize or Not to Normalize and What to Normalize to?, in Computational Intelligence in Electromyography Analysis, Ed. G. R. Naik, IntechOpen, Rijeka, chapter 7, doi:10.5772/49957.
https://doi.org/10.5772/49957

Hirokawa, S., M. Solomonow, Z. Luo, Y. Lu and R. D'ambrosia (1991), Muscular co-contraction and control of knee stability, **vol. 1**, no.3, pp. 199–208.

Kothera, C. S., M. Jangid, J. Sirohi and N. M. Wereley (2009), Experimental characterization and static modeling of McKibben actuators, **vol. 131**, no.9, p. 091010.

LaPrade, R. F., S. D. Smith, K. J. Wilson and C. A. Wijdicks (2015), Quantification of functional brace forces for posterior cruciate ligament injuries on the knee joint: an in vivo investigation, **vol. 23**, no.10, pp. 3070–3076.

Lee, S. J., K. J. Aadalen, P. Malaviya, E. P. Lorenz, J. K. Hayden, J. Farr, R. W. Kang and B. J. Cole (2006), Tibiofemoral Contact Mechanics after Serial Medial Meniscectomies in the Human Cadaveric Knee, **vol. 34**, no.8, pp. 1334–1344, doi:10.1177/0363546506286786, pMID: 16636354.
https://doi.org/10.1177/0363546506286786

Li, G., T. Rudy, M. Sakane, A. Kanamori, C. Ma and S.-Y. Woo (1999), The importance of quadriceps and hamstring muscle loading on knee kinematics and in-situ forces in the ACL, **vol. 32**, no.4, pp. 395–400.

Liu, W. and M. E. Maitland (2000), The effect of hamstring muscle compensation for anterior laxity in the ACL-deficient knee during gait, **vol. 33**, no.7, pp. 871–879.

Logan, M. C., A. Williams, J. Lavelle, W. Gedroyc and M. Freeman (2004), What really happens during the Lachman test? A dynamic MRI analysis of tibiofemoral motion, **vol. 32**, no.2, pp. 369–375.

Mori, M., K. Suzumori, M. Takahashi and T. Hosoya (2010), Very high force hydraulic McKibben artificial muscle with a p-phenylene-2, 6-benzobisoxazole cord sleeve, **vol. 24**, no.1-2, pp. 233–254.

Naghibi Beidokhti, H., D. Janssen, S. van de Groes, J. Hazrati, T. Van den Boogaard and N. Verdonschot (2017), The influence of ligament modelling strategies on the predictive capability of finite element models of the human knee joint, Journal of biomechanics, **vol. 65**, pp. 1–11.

Onishi, H., R. Yagi, M. Oyama, K. Akasaka, K. Ihashi and Y. Handa (2002), EMG-angle relationship of the hamstring muscles during maximum knee flexion, **vol. 12**, no.5, pp. 399–406.

Orthomen (2019), Orthomen OA Unloading Knee Brace - for Osteoarthritis & Preventive Protection from Knee Joint Pain/Degeneration - Lateral, united States of America.

Parween, R., D. Shriram, R. E. Mohan, Y. H. D. Lee and K. Subburaj (2019), Methods for evaluating effects of unloader knee braces on joint health: a review, Biomedical engineering letters, pp. 1–16.

Rachmat, H., D. Janssen, G. J. Verkerke, R. Diercks and N. Verdonschot (2016), In-situ mechanical behavior and slackness of the anterior cruciate ligament at multiple knee flexion angles, **vol. 38**, no.3, pp. 209–215.

Roche, E. (2019), Gripper for SDM fingers, [Online; accessed 1-September-2019]. https://softroboticstoolkit.com/book/pam-fabrication

Rudolph, K. S., M. E. Eastlack, M. J. Axe and L. Snyder-Mackler (1998), 1998 Basmajian Student Award Paper: Movement patterns after anterior cruciate ligament injury: a comparison of patients who compensate well for the injury and those who require operative stabilization, **vol. 8**, no.6, pp. 349–362.

Slater, L. V., J. M. Hart, A. R. Kelly and C. M. Kuenze (2017), Progressive changes in walking kinematics and kinetics after anterior cruciate ligament injury and reconstruction: a review and meta-analysis, **vol. 52**, no.9, pp. 847–860.

Sridar, S., Z. Qiao, N. Muthukrishnan, W. Zhang and P. Polygerinos (2018), A Soft-Inflatable Exosuit for Knee Rehabilitation: Assisting Swing Phase During Walking, Frontiers in Robotics and AI, **vol. 5**, p. 44, ISSN 2296-9144, doi:10.3389/frobt.2018.00044. https://www.frontiersin.org/article/10.3389/frobt.2018.00044

Sun, Y., Y. S. Song and J. Paik (2013), Characterization of silicone rubber based soft pneumatic actuators, in 2013 IEEE/RSJ International Conference on Intelligent Robots and Systems, Ieee, pp. 4446–4453.

Tomescu, S., R. Bakker, D. Wasserstein, M. Kalra, M. Nicholls, C. Whyne and N. Chandrashekar (2018), Dynamically tensioned ACL functional knee braces reduce ACL and meniscal strain, **vol. 26**, no.2, pp. 526–533, ISSN 1433-7347, doi:10.1007/s00167-017-4794-1. https://doi.org/10.1007/s00167-017-4794-1

Tondu, B. (2012), Modelling of the McKibben artificial muscle: A review, **vol. 23**, no.3, pp. 225–253, doi:10.1177/1045389X11435435. https://doi.org/10.1177/1045389X11435435

Tondu, B. and P. Lopez (2000), Modeling and control of McKibben artificial muscle robot actuators, **vol. 20**, no.2, pp. 15–38.

Toy, B. J., R. A. Yeasting, D. E. Morse and P. McCann (1995), Arterial supply to the human anterior cruciate ligament, **vol. 30**, no.2, p. 149.

Walden, M. (Oct 11, 2016), Hamstring Tendonitis, [Online; accessed 13-Sept-2019]. https://www.sportsinjuryclinic.net/sport-injuries/knee-pain/posterior-knee-pain/biceps-femoris-tendinopathy

Walter, M. (2016), Artificial Muscles To Bring Relief To Robotic Tenseness, [Online; accessed 1-September-2019]. https://hackaday.com/2016/06/06/

artificial-muscles-to-bring-relief-to-robotic-tenseness/

Wilson, C. (2018), ACL Knee injury, [Online; accessed 14-September-2019].
https://www.knee-pain-explained.com/ACL-knee-injury.html